



1 **Characterization of chromophoric dissolved organic matter in**
2 **lakes on the Tibet Plateau, China, using spectroscopic analysis**

3 Kaishan Song^{1#*}, Sijia Li^{2#}, Zhidan Wen¹, Lili Lyu¹, Yingxin Shang¹

4 ¹ Northeast Institute of Geography and Agroecology, CAS, Changchun, 130102, China

5 ² School of Environmental, Northeast Normal University, Changchun, 136000, China

6 # first co-authors

7 *authors correspondence should be addressed: songkaishan@neigae.ac.cn

8 **Abstract** Spatiotemporal variations in the characteristics of fluorescent dissolved
9 organic matter (FDOM) components from 63 lakes across the Tibet Plateau, China, are
10 examined using excitation-emission matrix spectra (EEM) and fluorescence regional
11 integration (FRI) from 2014 to 2017. Freshwater ($N=135$) and brackish water ($N=109$)
12 samples from 63 lakes were grouped according to salinity or electrical conductivity. In
13 order to compare results between the lakes, cumulative volumes beneath the EEM
14 values (ϕ_i , $i=I, II, III, IV, V$) were normalized to a DOC concentration of 1 mg/L. EEM-
15 FRI identified tyrosine-like (ϕ_I), tryptophan-like (ϕ_{II}), fulvic-like (ϕ_{III}), microbial
16 protein-like (ϕ_{IV}), and humic-like (ϕ_V) fluorescence regions, as well as their proportions
17 (P_i). Chromophoric dissolved organic matter (CDOM) absorption parameters,
18 fluorescence indices, average fluorescence intensities of the five fluorescent
19 components and total fluorescence intensities (ϕ_T) differed under spatial variation
20 among brackish and freshwater lakes (ANOVA, $p<0.05$). Principal component analysis
21 (PCA) was used to assess and group five normalized FDOM components for all of the
22 water samples. These results show that microbial protein-like (ϕ_{IV}), fulvic-like (ϕ_{III})
23 and humic-like (ϕ_V) have positive correlations ($R^2>0.79$, t -test, $p<0.01$), indicating that
24 these FDOM components may originate from similar sources. A correlation also exists



25 between normalized φ_i ($i=I, II, III, IV, V$) and DOC concentrations with a salinity $>19\%$
26 (averaged EC, $23764\mu\text{s cm}^{-1}$) (t -test, $p<0.01$), of which R^2 regression analysis showed
27 a decreasing tendency with EC. Similar correlations between $a(254)$ and DOC
28 concentrations (t -test, $p<0.01$) are also evident for sunshine hours > 2900 h.
29 Redundancy analysis (RDA) indicates that $a(254)$ and $a(350)$ have a correlation with
30 CDOM in brackish lakes. $a(254)$, HIX and $a(350)$ were also correlated with water
31 quality. Strong evapoconcentration, intense ultraviolet irradiance and landscape
32 features of the Tibet Plateau may be responsible for the FDOM characteristics identified
33 in this study.

34 Keywords: CDOM; Tibet Plateau; Fluorescence; Brackish lakes; FRI



35

36 **1. Introduction**

37 Inland lakes are a direct link between the land and atmospheric CO₂ pools and rivers,
38 and they are an indirect link between the oceans (via rivers). Inland lakes play an
39 important role in the transportation, transformation and storage of carbon from
40 terrestrially imported substances (Cole et al., 2007; Tranvik et al., 2009). Carbon flux
41 and biogeochemical processes of lakes have a significant influence on the global carbon
42 cycle, on the aquatic ecosystem, and they confer regional effects on climate (Battin et
43 al., 2009; Jiao et al., 2010; Ran et al., 2013; Carlson et al., 2011). However,
44 anthropogenic activities (i.e., industrial, agricultural and domestic sewage) can alter the
45 carbon balance and interfere with biogeochemical cycling of lakes, effects which can
46 be recorded in spatiotemporal variations of dissolved carbon within the catchment. It is
47 therefore important to investigate biogeochemical cycling of carbon in lakes in different
48 regions that have distinct properties (Cole et al., 2007; Falkowski et al., 2000).

49 The Tibet Plateau, commonly known as the ‘Third Pole’ or the ‘Asian water tower’,
50 possesses an average elevation over 4500 m, and contains the largest ice mass outside
51 the polar regions (Song et al., 2016). This region also contains the greatest number of
52 large-scale lakes and glaciers in the world. The total area of lakes on the Tibet Plateau
53 account for about 49% of the total lake area in China (Zhang et al., 2011). As of 2011,
54 there were 312, 104, 7 and 3 lakes with surface areas greater than 10 km², 100 km², 500
55 km² and 1000 km², respectively (Zhang et al., 2011). In addition, due to dry and thin
56 air with a low concentration of ozone in this area, there are strong Ultraviolet-B (UV-
57 B) radiation-penetration inhibiting properties (Ren et al., 1997). Prolonged sunshine
58 and the arid environment has resulted in a high number of lakes in this region having a
59 high salt content, or having a significant accumulation of dissolved organic carbon



60 (DOC). DOC and dissolved organic matter (DOM) contents contained in brackish or
61 saline lakes, particularly in arid and semi-arid regions, contribute to the relatively high
62 average DOC concentrations and carbon budget of inland waters (Song et al., 2013;
63 Tranvik et al., 2009; Wen et al., 2016). Due to its high altitude, arid environment, low
64 population density, urbanization, and economic development, the Tibet Plateau is
65 therefore of particular interest for climate change, environmental evolution and the
66 carbon cycle. There is also significant interest to investigate total DOM in brackish and
67 saline lakes across the Tibet Plateau.

68 DOM (typically $<0.45 \mu\text{m}$) represents one of the largest pools of organic carbon on
69 Earth (Hedges et al., 1992; McKnight et al., 2001). Chromophoric DOM (CDOM,
70 typically $<0.22 \mu\text{m}$), light-absorbing DOM in aquatic environments, originates from the
71 decomposition of algal by microorganisms (autochthonous), as well as through the
72 transport of the surrounding allochthonous environment (Singh et al., 2010; Zhang et
73 al., 2010). Chemical properties cause CDOM to absorb energy and re-emit it as
74 fluorescence (FDOM) (Helms et al., 2008; Stedmon et al., 2003; Zhang et al., 2010).
75 Due to the high selectivity and sensitivity of FDOM, absorption and fluorescence
76 spectroscopy has provided detailed insights into its composition and components
77 (Stedmon et al., 2003; Zhang et al., 2010). Multivariate statistical parameters and tools,
78 i.e., spectroscopic characterization (specific ultraviolet absorbance and spectral slope
79 ratio), excitation-emission matrix (EEM), humification index (*HIX*), fluorescence index
80 (*FI*), parallel factor analysis (PARAFAC) and fluorescence regional integration (FRI),
81 have been utilized to identify bio-geochemically meaningful components of CDOM
82 (Coble, 1996; Helms et al., 2008; Stedmon et al., 2003). EEM-PARAFAC and EEM-
83 FRI techniques can show dynamic and detailed components of FCDOM for each EEM,
84 techniques which have been widely used in aquatic environmental dynamics (source



85 and fate) (Chen et al., 2003; Zhang et al., 2010; Zhao et al., 2017). Compared to other
86 fluorescence tools, EEM-FRI (a quantitative technique) can integrate the volumes
87 beneath defined by regions of EEM largely based on supporting literature (Chen et al.,
88 2003). This is related to all of the wavelength ranges of different fluorescence peaks in
89 each EEM, and covers continuous fluorescence intensity at excitation-emission
90 wavelength of divided regions for further analysis (Chen et al., 2003).

91 It is believed that the high altitude and arid environment of the Tibet Plateau could
92 have an influence on CDOM in brackish and saline lakes. These influences may affect
93 DOC accumulation, result in a high photochemical degradation rate due to prolonged
94 sunshine, decrease anthropogenic CDOM inputs, and result in an accumulation of
95 nutrients in lake catchment areas (Spencer et al. 2012; Yao et al., 2011; Song et al.,
96 2017). Although CDOM optical characteristics and their effect on carbon budget
97 contribution have been reported in plateaus and high-mountain lakes (Wen et al., 2016;
98 Zhang et al., 2010), little is currently known about CDOM in the Tibet Plateau. Analysis
99 in this area could reveal a natural state of composition, sources, dynamics, and fate of
100 CDOM by comparing results with other brackish and saline lakes with high
101 eutrophication rates due to increased terrestrial nutrient input. Based on previous
102 studies, our investigation examines sources and fate of CDOM in brackish (31 lakes)
103 and saline lakes (32 lakes) across the Tibet Plateau using EEM-FRI. The study
104 objectives are to: (1) characterize the similarities and differences in CDOM absorption
105 and components among the 63 lakes with similar climatic, hydrologic and geological
106 conditions using EEM-FRI technology; (2) investigate and evaluate spatial dynamics
107 of each fluorescence component using EEM-FRI; (3) link FDOM by EEM-FRI to
108 CDOM absorption and fluorescence parameters, and to water quality; and (4) assess the
109 effects on FDOM by EEM-FRI caused by salinity, solar radiation and land cover.



110 **2. Materials and Methods**

111 **2.1 Overview of the Tibet lakes**

112 As the largest and most extensive plateau in the world, the Tibet Plateau covers an area
113 in China of about 2.5 million km², having an average elevation of more than 4500 m
114 above sea level (Zhang et al., 2011). Lakes on the Tibeta Plateau are typically formed
115 due to erosion and melting of glaciers, geological tectonic activity (fault and
116 depression), barriers present on the land-surface, or due to melting on hot spots etc. The
117 majority of these lakes are sensitive to global climate change (Liu and Chen, 2000; Qin
118 et al., 2009). Due to the diverse climate (some airflows of tropospheric tropical easterly,
119 subtropical westerly, and southwestern monsoon from the Indian Ocean) and complex
120 topography (numerous different broad basins or valleys with high mountain ranges) in
121 this area, annual precipitation ranges from 100 to 1300 mm. The majority of
122 precipitation occurs during the summer period (June to September). Solar UV radiation
123 in this area is strong due to dry and thin air, having a low ozone concentration (Ren et
124 al., 1997). In the winter the climate is dominated by cold and dry westerly winds which
125 are more pronounced with elevation. During the winter, the northwestern area of the
126 plateau (where average elevation exceeds 5000 m) is the coldest, having average
127 temperatures around -40 °C (Song et al., 2016). Owing to diverse climatic patterns,
128 topographical patterns and few anthropogenic activities, the carbon cycle, climate
129 change and environment evolution over the Tibet Plateau has seen an increase in interest
130 recently (Zhao et al., 2017; Song et al., 2017).

131 **[Insert Figure 1 about here]**

132 **2.2 Field sampling**

133 A total of 244 water samples were collected from 63 lakes across the Tibet Plateau from



134 2014 to 2017. Sample locations for each lake were recorded using a GPS receiver (Table
135 S1 and Fig. 1). Water samples were collected from lake surfaces (0-50 cm) in 1 L acid-
136 cleaned plastic bottles. The collected water samples were filtered through a pre-
137 combusted Whatman GF/F filter (0.7 μm) and then further filtered through a pre-rinsed
138 25 mm Millipore membrane cellulose filter (0.22 μm) into brown plastic bottles.
139 Samples were prepared for DOC analysis by being filtered through a pre-combusted
140 Whatman GF/F filter (0.45 μm) under a low vacuum. The filtered samples were stored
141 at 4°C and transported to the laboratory for CDOM absorption and fluorescence
142 analysis within 2 days.

143 **2.3 Water quality measurements**

144 Electrical conductivity (EC) and pH were measured using a portable multi-parameter
145 water quality analyzer (YSI EXO1, US). DOC concentrations were determined by high-
146 temperature catalytic oxidation (680 °C) using a total organic carbon analyzer (TOC-
147 VCPN, Shimadzu, Japan). Potassium hydrogen phthalate was used in this analysis as a
148 reference. Chlorophyll a (Chl-a) analysis was undertaken by initially filtering the water
149 samples through Whatman cellulose acetone filters (0.45 μm) before being extracted
150 with 90% acetone and measured at 664, 647, 630 and 750 nm wavelengths using a
151 Shimadzu UV-2006 PC spectrophotometer. Total nitrogen (TN) and Total phosphorus
152 (TP) were measured following methods highlighted in standard methods
153 (APHA/AWWA/WEF, 1998).

154 **2.4 CDOM absorption measurements**

155 Absorption spectra of filtered samples were measured between 200 and 800 nm at 1 nm
156 increments using a Shimadzu UV-2006 PC spectrophotometer with a 1 cm (or 5 cm)
157 quartz cuvette and Milli-Q water as a reference. The absorption coefficient a_{CDOM} was



158 calculated from the measured sample optical absorption $a(\lambda)$:

$$159 \quad a_{\text{CDOM}}(\lambda) = 2.303 \text{OD}(\lambda) / \gamma \quad (1)$$

160 where, $\text{OD}(\lambda)$ is the corrected optical density at wavelength λ ; γ is the cuvette path
161 length (0.01 or 0.05 m); and the factor of 2.303 converts the results from a base 10 to a
162 base natural logarithm (Zhang et al., 2011). The SUVA_{254} , $\text{S}_{275-295}$ and M ($\text{E}_{250}:\text{E}_{365}$)
163 were used to characterize CDOM features (Helms et al., 2008).

164 2.5 Excitation-emission matrix (EEM) fluorescence

165 Three-dimensional excitation-emission matrix (EEM) spectra of CDOM were
166 measured at room temperature (20 ± 2 °C) using a Hitachi F-7000 fluorescence
167 spectrometer with a 700 volt xenon lamp. Scanning band pass widths of excitation and
168 emission spectra were obtained using wavelengths of 220-450 nm (with intervals of 5
169 nm) and 250-600 nm (1 nm intervals), respectively, with a scanning speed of 2400
170 $\text{nm} \cdot \text{min}^{-1}$. A Milli-Q water blank was analyzed, the result of which was subtracted from
171 the resulting EEM of the water sample spectrum to eliminate Raman scatter peaks. In
172 order to eliminate the inner filter effect, the EEMs were normalized by subtracting the
173 integral area under the curve of the Milli-Q water Raman peak according to the methods
174 recommended by Zhang et al. (2010) and Zhou et al. (2016). These EEM spectra were
175 then calibrated in quinine sulfate units (QSU) (Lawaetz and Stedmon, 2009).

176 The fluorescence indices FI_{370} and FI_{310} , defined as $\text{Ex}/\text{Em} = (370/450$
177 $\text{nm}) / (370/500 \text{ nm})$ and $\text{Ex}/\text{Em} = (310/380 \text{ nm}) / (310/430 \text{ nm})$, introduced by McKnight
178 et al. (2001), were used to characterize CDOM source. FI_{370} is used to distinguish fulvic
179 acids derived from terrestrial ($FI_{370} < 1.4$) and microbial ($FI_{370} > 1.9$) sources, and FI_{310}
180 is used to distinguish autochthonous ($FI_{310} < 0.7$), autochthonous biological activity
181 ($FI_{310} > 0.8$) and intermediate autochthonous ($0.7 < FI_{310} < 0.8$) (Zhang et al., 2010). The
182 humification index (HIX) was calculated from fluorescence EEMs, as indices for the



183 humification degree and DOM sources (Huguet et al., 2009). Further details of these
 184 methods are provided in Zhang et al. (2010).

185 2.6 EEM fluorescence regional integration

186 EEM Fluorescence Regional Integration (EEM-FRI) divides EEM boundaries into five
 187 regions associated with humic-like, tyrosine-like, tryptophan-like or phenol-like
 188 organic compounds, based on the findings of Chen et al. (2003). Fluorescence peaks at
 189 $\text{Ex} < 250$ nm and $\text{Em} < 350$, defined as Regions I and II, relate to aromatic proteins such
 190 as tyrosine. Peaks at shorter $\text{Ex} < 250$ nm and longer $\text{Em} > 350$ nm are fulvic acid-like
 191 materials, deemed as Region III. Peaks at intermediate 250 nm $< \text{Ex} < 280$ nm and
 192 $\text{Em} < 380$ nm are microbial protein-like, defined as Region IV. Peaks at longer $\text{Ex} > 280$
 193 nm and $\text{Em} > 380$ nm are related to humic acid-like organics, denoted as Region V. The
 194 integrated area beneath the EEM spectra can be calculated using:

$$195 \quad \varphi_i = \int_{\text{ex}} \int_{\text{em}} I(\lambda_{\text{ex}} \lambda_{\text{em}}) \Delta \lambda_{\text{ex}} \Delta \lambda_{\text{em}} \quad (2)$$

196 where, $\Delta \lambda_{\text{ex}}$ is Ex (interval 5 nm); $\Delta \lambda_{\text{em}}$ is Em (interval 1 nm); $I(\lambda_{\text{ex}}, \lambda_{\text{em}})$ is fluorescence
 197 intensity at each EEM pair; and i represents the regions of EEM divided by EEM-FRI.
 198 The cumulative volume in the five regions beneath the EEM can be calculated using φ_T
 199 ($i = \text{I, II, II, IV, V}$; unit: nm):

$$200 \quad \varphi_{T,n} = \sum_{i=1}^5 \varphi_{i,n} \quad (3)$$

201 where, n represents the numbers of cumulative regions in the five regions. The
 202 cumulative volume beneath the EEM (φ_i and φ_T) values were normalized to per unit of
 203 DOC concentration (in mg/L) for comparison of EEMs from different sources. The unit
 204 of DOC-normalized EEM-FRI is $\text{QSU} \cdot \text{nm}^2 \cdot [\text{mg/LC}]^{-1}$. The percent fluorescence
 205 response in a specific region ($P_{i,n}$, $i = \text{I, II, II, IV, V}$) was calculated as:

$$206 \quad P_{i,n} = \frac{\varphi_{i,n}}{\varphi_{T,n}} \times 100\% \quad (4)$$



207 2.7 Statistical analysis

208 Statistical analyses, regression and correlation analyses were performed using SPSS
209 16.0 (Statistical Program for Social Sciences) to examine the relationships between
210 variations (CDOM absorption and fluorescence parameters) among lakes. Significance
211 levels are reported as non-significant (NS) ($p > 0.05$), significant (*, $0.05 > p > 0.01$) or
212 highly significant (**, $p < 0.01$). Redundancy analysis (RDA) and principal components
213 analysis (PCA) was undertaken using CANOCO 4.5 from two principal components
214 analyses (Microcomputer Power, Ithaca, NY, USA).

215 3. Results

216 3.1 Biogeochemical characteristics

217 Water quality parameters (TN, TP, Chl-a, TSM, pH, EC, turbidity and salinity) for the
218 63 lakes (244 water samples) are shown in Table 1. Thirty one lakes were classified as
219 brackish ($N=109$; 35‰ > salinity > 1‰) and 32 lakes were classified as freshwater
220 ($N=135$; salinity < 1‰). The average values of all water quality parameters in each lake
221 were calculated and selected to represent overall water quality of the lake.
222 Concentrations of TN (average, $2.31 \pm 2.64 \text{ mg L}^{-1}$), TP (average, $0.04 \pm 0.03 \text{ mg L}^{-1}$)
223 and Chl-a (average, $1.45 \pm 2.65 \text{ } \mu\text{g L}^{-1}$) were relatively low in fresh lakes ($N=135$),
224 coinciding with low turbidity. Brackish lakes, having a eutrophic state, recorded high
225 Chl-a (average, $2.57 \pm 5.73 \text{ } \mu\text{g L}^{-1}$), TN (average, $4.54 \pm 4.32 \text{ mg L}^{-1}$) and TP (average,
226 $0.45 \pm 1.35 \text{ mg L}^{-1}$), results related to their high salt (average, $6.01 \pm 5.59 \text{ } \text{‰}$) and EC
227 (average, $8880.24 \pm 8235.9 \text{ } \mu\text{S cm}^{-1}$) contents. The water quality parameters of the
228 trophic states were slightly higher than the average values for brackish lakes in
229 northeastern China (average, TP=0.11 mg L^{-1} and TN=4.07 mg L^{-1} ;) in Northeast of
230 China (Zhao et al., 2017), and lakes (average, TP=0.033 mg L^{-1} and TN=0.59 mg L^{-1} ;)



231 in Yungui Plateau of China (Zhang et al., 2010), and lower than those in Hulun Lake
232 (average, TP=1.52 mg L⁻¹ and TN=4.58 mg L⁻¹; Wen et al., 2016). Zhang et al. (2010)
233 found that, with an increase in altitude (> 4000 m), oligotrophic lakes increased due to
234 the natural changes in catchment properties and low human activities. However, for
235 terminal lakes with less anthropogenic density, there is an accumulation of nutrients
236 generally derived from allochthonous substances.

237 **[Insert Table 1 about here]**

238 High concentrations of DOC in brackish waters were found to accumulate in
239 lakes with high salinity concentrations (Fig. 2a). DOC values for the brackish lakes
240 were also found to be variable, ranging from 0.27 mg L⁻¹ in Lake XRC to 164.8 mg L⁻¹
241 in Lake CCL, with a mean DOC of 35.69 (± 43.52) mg L⁻¹ (Fig. S1). Mean DOC
242 concentrations in the fresh lakes were 7.94 ± 12.05 mg L⁻¹, recording lower values than
243 those in brackish lakes. These results are in agreement with the findings of Song et al.
244 (2013), Zhao et al., (2016) and Wen et al (2016) for brackish lakes in arid and semi-arid
245 regions. Although brackish lakes have high spatial heterogeneity, our results indicate
246 that decreasing salinity generally coincides with DOC concentrations (Fig. 2b). In
247 addition, owing to UV-B radiation-penetration inhibiting properties in the Tibet Plateau
248 (Ren et al., 1997), the tendency linear equation of average DOC concentration showed
249 a decreased trend with increasing elevation (Fig. 2a). However, variations in DOC
250 concentrations can also be explained by DOC flux related to physical/chemical
251 properties, hydrology, and land use/land cover within a specific drainage watershed for
252 each lake (Heinz et al., 2015; Wen et al., 2016).

253 **[Insert Figure 2 about here]**

254 **3.2 CDOM absorption**

255 Previous studies have indicated that high salinity could have a direct or indirect impact



256 on water quality, and they highlighted different structures and composition of DOM
257 (Waiser and Robarts, 2000; Song et al., 2013; Zhang et al., 2010). Generally, Helms et
258 al. (2008) and Weishaar et al. (2003) showed that the absorption coefficient $a(350)$ is
259 seen as a proxy to characterize CDOM concentration. $a(350)$ absorption coefficients in
260 our study ranged from 0.09–8.45 m^{-1} and 0–13.49 m^{-1} for brackish and fresh lakes, with
261 mean values of 2.38 (± 3.14 SD) m^{-1} and 1.74 (± 1.99 SD) m^{-1} , respectively (Fig. 3).
262 These values were found to be significantly different from each other (ANOVA,
263 $p < 0.05$). $a(254)$ represents the optical properties of DOC aromaticity, and SUVA_{254} (the
264 ratio of $a(254)$ and DOC) can be used to characterize the optical properties of DOC
265 aromaticity (Helms et al., 2008; Spencer et al., 2012). Higher SUVA_{254} values are
266 related to allochthonous-dominated sources, having a higher percentage of DOC
267 aromaticity and microbial-dominated substances in DOC; lower SUVA_{254} values
268 indicate the opposite (Spencer et al., 2012; Weishaar et al., 2003). Mean SUVA_{254} values
269 ranged from 1.47 (± 2.55 SD) $\text{mg C}^{-1} \text{m}^{-1}$ in brackish lakes to 2.29 (± 1.36 SD) mg C^{-1}
270 m^{-1} in fresh lakes (Fig. 2). ANOVA analysis indicated there are significant differences
271 ($p < 0.05$) between SUVA_{254} values for brackish and fresh lakes. SUVA_{254} values for
272 brackish lakes recorded lower values than those recorded in terminal water on the Inner
273 Mongolia Plateau (Brackish, $\text{SUVA}_{254} = 1.90 \pm 0.57 \text{ mg C}^{-1} \text{m}^{-1}$; Fresh,
274 $\text{SUVA}_{254} = 2.74 \pm 1.08 \text{ mg C}^{-1} \text{m}^{-1}$) or in brackish lakes of northeastern China (2.8–5.7 mg
275 $\text{C}^{-1} \text{m}^{-1}$) (Zhao et al., 2016; Wen et al., 2016). In this study, the lower SUVA_{254} values
276 in the brackish lakes indicated that aromatic moieties of CDOM in this environment
277 were lower than those in fresh lakes, or other brackish environments in China. These
278 differences are due to the effect of photo-degradation and microbial degradation, with
279 prolonged water residence times.

280 For brackish water lakes, $M (E_{250}:E_{365})$ ranged from 6.82 in Dajiacuo Lake (DJC)



281 to 74.7 in Gemangcuo Lake (GMC), having an average value of 28.3 ± 20.3 (Fig. 3)
282 across all brackish lakes. Results for M ($E_{250}:E_{365}$) in fresh lakes ranged from 5.7 in
283 Tongzecu Lake (TZC) to 89.5 in Lang'angcuo Lake (LAC), having an average value
284 of 16.27 ± 20.6 . This suggests a significant difference (ANOVA, $p < 0.05$) between fresh
285 and brackish waters in M ($E_{250}:E_{365}$). The spectral $S_{275-295}$ (275–295 nm) was used to
286 represent DOM molecular weight, with higher values signifying lower average
287 molecular weights of DOC (Helms et al., 2008). Then $S_{275-295}$ can be regarded as an
288 indicator for terrestrial DOC percentage (Gonnelli et al., 2013). As shown in Figure 3,
289 the higher $S_{275-295}$ values ($0.0380 \pm 0.009 \text{ nm}^{-1}$) in brackish lakes than those in presented
290 in fresh lakes ($0.0324 \pm 0.01 \text{ nm}^{-1}$; Fig. 3), indicating lower average molecular weight
291 of DOM. This result showed a significant difference between fresh and brackish lakes
292 (ANOVA, $p < 0.05$). This implies that chromophores associated with high molecular
293 weight were destroyed by chemical bond rupture into low molecular weight pool in the
294 photolysis process with a prolonged hydraulic retention time and irradiation (McKnight
295 et al., 2001). The difference in CDOM absorption parameters is probably associated to
296 spatial variations influencing terrestrial inputs from soil and microbial activities due to
297 plant decay.

298 **[Insert Figure 3 about here]**

299 **3.3 EEM-FRI components**

300 EEM spectra of CDOM referred to the major fluorescent components and location
301 information identified using the peak-picking method of Coble (1996) and PARAFAC
302 from previous studies (Stedmon et al. 2003; Kowalczyk et al., 2010). Typical EEM
303 spectra of CDOM for four water samples obtained from brackish and fresh lakes in the
304 Tibet Plateau are shown in Figure 4 (a-d). Traditional EEM fluorescence peaks, i.e.,
305 phytoplankton production ('N' peak), tyrosine-like ('B' peak), humic-like ('M' peak)



306 and tryptophan-like ('T' peak) were observed in the 244 EEM spectra (Coble, 1996).
307 According to Chen et al. (2003), EEM-FRI divides the EEM signal into five regions (I,
308 II, III, IV and V; Fig. 3a). In the Tibet Plateau, these regions varied with changes in
309 intensity of the five marked fluorescence fractions between brackish lakes and the fresh
310 lakes. EEM-FRI results from the lakes were used to demonstrate CDOM fluorescence
311 characteristics. The excitation-emission area volumes φ_i ($i= I, II, III, IV, V$) and their
312 proportion to total fluorescence intensity P_i ($i= I, II, III, IV, V$) for the five different
313 regions are shown in Figure 4 (e and f), respectively. A significant difference (ANOVA,
314 $p<0.05$) of total fluorescence intensity φ_T was observed between the brackish and fresh
315 lakes. φ_T ranged from 1.94×10^8 nm to 3.5×10^{10} nm for brackish lakes, having an
316 average of 1.44×10^{10} nm ($\pm 8.1 \times 10^9$ SD), and it ranged from 3.54×10^8 nm to $3.5 \times$
317 10^{10} nm for freshwater lakes, with an average of 1.38×10^{10} nm ($\pm 7.9 \times 10^9$ SD). For
318 both lake types, the area volume of φ_i in the five integrated regions identified by EEM-
319 FRI were in the order of: φ_V (Humic-like) $>$ φ_{III} (Fulvic-like) $>$ φ_{IV} (Microbial protein-
320 like) $>$ φ_I (Tyrosine-like) $>$ φ_{II} (Tryptophan-like). This result indicates that the
321 allochthonous humic-like and fulvic-like materials are predominate in these DOM, and
322 the content of protein-like materials and phenolic compounds were low. Furthermore,
323 a significant difference for the fluorescence intensities of humic-like φ_V and fulvic-like
324 φ_{III} was found in brackish lakes and fresh lakes (ANOVA, $p<0.05$). The fluorescence
325 intensities with φ_V accounting for $P_V=62.4\%$ (± 14.6 SD) in brackish lakes ranged from
326 34.1% in Gemangcuo Lake (GMC) to 96.8% in Chuocuolong Lake (CCL). Then fresh
327 lakes recorded a range of 32.8% (Garencuo Lake; GRC-2) to 87.5% (Cuolongque Lake;
328 CLQ), having an average P_V of 53.7% (± 13.0 SD). This result indicates that humic-like
329 substances both in brackish and fresh lakes dominated fluorescence intensities. In
330 addition, the φ_{III} (fulvic-like) fluorescence intensities also showed a significant



331 difference (ANOVA, $p < 0.05$) between P_{III} in fresh lakes (24.8%; ± 7.4 SD) and those in
332 brackish lakes (15.9 %; ± 8.8 SD). The fluorescence intensities for φ_{IV} (microbial
333 protein-like) accounted for a greater proportion in brackish lakes (P_{IV} of 15.5%; ± 8.2
334 SD) than in fresh lakes (12.5%; ± 6.8 SD). These results demonstrated that the
335 fluorescence intensities of the five components φ_i ($i = I, II, II, IV, V$) and the relative
336 proportions to the total fluorescence intensities P_i ($i = I, II, II, IV, V$) differed in brackish
337 and fresh lakes.

338 **[Insert Figure 4 about here]**

339 **3.4 Normalized EEM-FRI components and fluorescence indices**

340 With various hydrological, geographical and climatic characteristics, the fluorescence
341 of CDOM components in different lakes shows spatial heterogeneity. The water
342 samples collected from each lake were combined to examine spatial variation. In order
343 to eliminate the influence of spatial heterogeneity, the cumulative volumes beneath the
344 EEM (φ_i) values were normalized to a DOC concentration of 1 mg L⁻¹. The average
345 normalized total fluorescence intensities φ_T in brackish lakes was 1.1×10^9 QSU-nm²-
346 [mg L⁻¹ C] (± 8.8 SD), with a maximum value of 3.3×10^9 QSU-nm²-[mg L⁻¹ C] in
347 Gongzhucuo Lake (GZC) and a minimum value of 4.8×10^7 QSU-nm²-[mg L⁻¹ C] in
348 Qinghaihu Lake (QHH). Results for the fresh lakes showed that φ_T ranged from 2.1
349 $\times 10^7$ QSU-nm²-[mg L⁻¹ C] in Tongzecu Lake (TZC) to 9.5×10^9 QSU-nm²-[mg L⁻¹ C]
350 in Wurucuo Lake (WRC), having an average φ_T of 3.3×10^9 QSU-nm²-[mg L⁻¹ C] (± 2.6
351 SD). There was a significant difference of normalized total fluorescence intensities φ_T
352 in brackish and fresh lakes (ANOVA, $p < 0.001$), which is opposite to the non-
353 normalized EEM-FRI result in Figure 4e. This difference may be attributed to DOC
354 accumulation in terminal brackish lakes, having a prolonged hydraulic retention time



355 and irradiation, and the presence of a greater volume of colorless DOC (Table S1). By
356 contrast, it can be seen that the inflow rivers of a certain lake generally showed lower
357 DOC concentrations (Fig. S2). Although photochemistry due to strong UV-B caused
358 the different composition of CDOM, allochthonous substances are important for the
359 accumulation of DOC in brackish lakes.

360 In addition, the normalized volumes φ_i in the five integrated regions identified by
361 EEM-FRI also presented normalized φ_V (humic-like), φ_{III} (fulvic-like) and φ_{IV}
362 (microbial protein-like), these being more predominate in CDOM than φ_I (tyrosine-like)
363 and φ_{II} (tryptophan-like). Percentage distributions (P_i) of EEM-FRI extracted FDOM in
364 brackish and fresh lakes also showed significant differences (ANOVA, $p < 0.001$).
365 Normalized humic-like (φ_V) and fulvic-like (φ_{III}) were terrestrial sources, accounting
366 for $P_{III+V} = 77.7\%$ (± 10.1 SD) in brackish lakes and 77.7% (± 7.3 SD) in fresh lakes.
367 Protein-like fluorescence, including tyrosine-like and tryptophan-like (φ_{I+II}), recorded a
368 greater proportion in brackish water ($P_{I+II} = 6.47\%$; ± 2.6 SD) than in fresh lakes (P_{I+II}
369 $= 22.3\%$; ± 4.0 SD) (Fig. 5c and d). Although autochthonous and microbial occupied
370 small proportions of normalized volumes φ_T , FDOM in brackish lakes generally
371 indicated more allochthonous inputs.

372 **[Insert Figure 5 about here]**

373 As shown in Fig. 6, the average values of the fluorescence indices FI_{370} and FI_{310}
374 introduced by McKnight et al. (2001) were derived to characterize CDOM sources in
375 the Tibet Plateau (Fig. 6). FI_{370} in brackish lakes ranged from 0.11 (Peikucuo Lake;
376 PKC) to 1.93 (Chuocuo Lake; CCL), with a mean value of 0.64 (± 0.51 SD); FI_{310}
377 ranged from 0.58 (PKC) to 1.93 (Gemangcuo Lake; GMC), having a mean value of
378 1.14 (± 0.36 SD). In contrast, fresh lake results ranged from 0.11 (Taruocuo Lake; TRC)
379 to 2.87 (Weizhi-1 Lake; WZ-1), with a mean value of 0.79 (± 0.75 SD) and from 0.57



380 (WZ-1) to 2.38 (La'angcuo Lake; LAC), with a mean value of 1.04 (\pm 0.43 SD), for
381 FI_{370} and FI_{310} , respectively. Average FI_{370} (<1.4) and FI_{310} (>0.8) in most brackish and
382 fresh lakes indicated that CDOM sources were derived from terrestrial humic-like
383 substances and autochthonous biological activity. There may be no differences between
384 FI_{310} and FI_{370} , signifying no difference for CDOM sources between brackish and fresh
385 lakes (ANOVA, $p>0.05$). However, average HIX (3.15 ± 3.5) in fresh lakes showed a
386 higher degree of humification than in brackish lakes (average HIX of 1.8 ± 1.7).

387 **[Insert Figure 6 about here]**

388 **3.5 PCA of normalized EEM-FRI components**

389 PCA (principal component analysis) was undertaken to calculate the relative scores of
390 normalized cumulative volume φ_i by EEM-FRI, and to assess the spatial distributions
391 of water samples in brackish and fresh lakes. Our results indicate that PCA factor 1 and
392 factor 2 axes (Fig. 7) could explain 92.8% of total variance, and they account for 66.9%
393 and 25.9%, respectively. The Kaiser-Meyer-Olkin result showed that the statistical
394 magnitude was larger than 0.8, and that the five normalized EEM-FRI fluorescent
395 components exhibited positive factor 1 loadings (Fig. 7a). Factor analysis showed PAC
396 factor 1 and factor 2 to be associated with five cumulative volumes φ_i ($i=I, II, III, IV,$
397 V) in a linear formula. Factor 1 and factor 2 were expressed as:

$$398 \text{ factor 1} = -0.543\varphi_I - 1.35\varphi_{II} + 0.788\varphi_{III} + 0.856\varphi_{IV} + 0.98\varphi_V$$

$$399 \text{ factor 2} = 0.899\varphi_I + 1.78\varphi_{II} - 0.559\varphi_{III} - 0.636\varphi_{IV} - 0.774\varphi_V.$$

400 φ_{III} (fulvic-like), φ_V (humic-like) and φ_{IV} (microbial protein-like) showed a positive
401 factor 1 loading, and concurrently showed negative factor 2 loading. This correlation
402 result indicated that PCA in our study could separate normalized cumulative volume φ_i
403 by EEM-FRI into two groups: Group 1 (φ_{III} , fulvic-like; φ_V , humic-like; φ_{IV} , microbial



404 protein-like) and Group 2 (ϕ_I , tyrosine-like; ϕ_{II} , tryptophan-like). This finding was
405 contrary to the results of Zhao et al. (2017), Yao et al. (2011) and Yamashita et al., (2010)
406 from other water bodies. Differences in results from our study and previous
407 investigations may be due to the majority of the microbial protein-like fluorescence of
408 CDOM in lakes in our study being derived from terrestrial microbial decomposition.
409 The spatial variation of PCA factors 1 and 2 scores for all water samples is shown in
410 Figure 7b. Water samples from brackish lakes were mainly distributed in the range of -
411 1 to 1 for both PCA factor scores. This finding confirms that the contributions of
412 allochthonous substances (including microbial protein-like) were obvious in brackish
413 lakes. Differences in FDOM results are likely to be due to spatial variations influencing
414 terrestrial inputs from soil and microbial activities from plant decay. However, PCA
415 scores from areas of fresh lakes were sporadic, signifying that normalized cumulative
416 volume ϕ_i were affected by regional hydrological and geographical lake conditions.

417 **[Insert Figure 7 about here]**

418 **3.6 Correlation analysis of CDOM spectroscopic indices**

419 In general, there was strong correlation between tyrosine-like ϕ_I and tryptophan-like ϕ_{II}
420 in fresh ($R^2=0.86$, $N=135$; t -test, $p<0.01$) and brackish lakes ($R^2=0.80$, $N=109$; t -test,
421 $p<0.01$), suggesting that they may have similar sources (Fig. 8a). A moderate
422 correlation between ϕ_I and microbial protein-like ϕ_{IV} was observed in brackish lakes
423 ($R^2=0.70$, $N=109$; t -test, $p<0.01$), and a weak correlation was recorded in fresh lakes
424 ($R^2=0.57$, $N=135$; t -test, $p<0.01$) (Fig. 8b), demonstrating that parts of the two FRI
425 fluorescent components may have some common sources in brackish lakes. However,
426 strong correlations between tryptophan-like ϕ_{II} and microbial protein-like ϕ_{IV} were not
427 observed (Fig. 8c), a finding that is consistent with the results of Chen et al. (2003) and



428 Zhao et al. (2017). This lack of correlation may be due to the sources of the three protein
429 fluorescence materials (tyrosine-like, tryptophan-like and microbial protein-like) being
430 independent in fresh lakes. Furthermore, EEM can be divided into two groups in the
431 PCA results (Fig. 7), and there was a positive correlation between the total normalized
432 cumulative volume $\varphi_{III&IV&V}$ and $\varphi_{I&II}$ ($R^2 = 0.76$, $N = 109$; t -test, $p < 0.01$) in brackish
433 lakes (Fig. 8d). Then a weak correlation in fresh lakes ($R^2 = 0.54$, $N = 135$; t -test, $p <$
434 0.01). It indicated that the autochthonous substances and they affected by
435 microorganism activity in brackish lakes was not strong. Arts et al. (2000) reported that
436 increasing salinity could limit the microbial activity by reduce the cell permeability. In
437 addition, moderate correlations between the $a(350)$, FI_{370} and HIX were observed in the
438 fresh lakes ($R^2 > 0.66$, $N = 135$; t -test, $p < 0.01$) (Fig. 8 e and f), showing that FI_{370} and
439 HIX represented similar indications in CDOM sources for most fresh lakes. This result
440 was consistent with the findings of Zhang et al. (2010) and Zhao et al. (2016). In
441 brackish lakes, $a(350)$ and HIX showed a more moderate correlation ($R^2 = 0.65$, $N = 109$;
442 t -test, $p < 0.01$).

443 **[Insert Figure 8 about here]**

444 **3.7 Correlation between CDOM and water quality**

445 Redundancy analysis (RDA) between water quality parameters for the brackish and
446 fresh lakes (Fig. 9) showed that the forward selected environment explanatory variables
447 (CDOM absorption and fluorescence; $a(254)$, $a(350)$, $S_{275-295}$, $SUVA_{254}$, $M(E_{250}:E_{365})$,
448 FI_{310} , FI_{370} , HIX and φ_i ($i = I, II, III, IV, V$)), could explain the variability of species
449 variables (water quality parameters; DOC, Chl-a, TN, TP, salinity and turbidity).
450 Species–environment correlations of brackish and freshlakes were 0.43 and 0.33,
451 respectively. For brackish lakes ($N = 109$), the first two RDA axes accounted for 86.3%



452 of total water quality parameter variability (axis one, 48 %; axis two, 38.3 %).
453 Coefficients between environmental variables with RDA axes indicated that $a(254)$,
454 $a(350)$ and HIX were correlated with CDOM, followed by $M(E_{250}:E_{365})$ and $S_{275-295}$. For
455 the fresh lakes ($N=135$), the first two RDA axes accounted for 82.4 % of total variability
456 (axis one, 66.7 %; axis two, 15.7 %). $a(254)$, HIX and $a(350)$ were correlated with water
457 quality, followed by FI_{370} and ϕ_{IV} . The CDOM absorption $a(254)$ can generally
458 characterize DOC aromaticity and CDOM concentration (Baker, 2001).

459 **[Insert Figure 9 about here]**

460 In addition, regression analysis was undertaken between DOC concentration and
461 normalized cumulative volume ϕ_i ($i=I, II, III, IV, V$) for all water samples (Table 2).
462 Salinity of the brackish lakes was divided into four parts: salinity $>19\text{‰}$ (average EC
463 $23764 \mu\text{s cm}^{-1}$), salinity $>7\text{‰}$ (average EC $10945 \mu\text{s cm}^{-1}$), salinity $>2\text{‰}$ (average EC
464 $5708 \mu\text{s cm}^{-1}$) and salinity $<1\text{‰}$ (average EC $2119 \mu\text{s cm}^{-1}$). Salinity $<1\text{‰}$ was
465 consistent with that of fresh lakes (average EC $586 \mu\text{s cm}^{-1}$). There were moderately
466 strong negative correlations between the normalized cumulative volume ϕ_i ($i=I, II, IV,$
467 V) and DOC concentration, with R^2 ranging from 0.51 to 0.73. This result suggests that
468 parts of the FDOM components and DOC potentially derived from common sources in
469 brackish lakes (salinity $>19\text{‰}$ or averaged EC $23764 \mu\text{s cm}^{-1}$). In particular, R^2 values
470 showed a consistent decreasing tendency with salinity (EC), suggesting that DOC with
471 high salinity (EC) was dominant with allochthonous substances. The link of the five
472 FDOM components to DOC was complicated due to various hydrological, geographical
473 and climatic characteristics.

474 **[Insert Table 2 about here]**

475 **4. Discussion**



476 4.1 The effect of EC/salinity

477 Previous studies have reported that DOC concentrations in inland waters showed a
478 decreased tendency with the prolongation of water residence times in humid regions
479 due to prolonged photobleaching and possible dilution (Curtis and Adams, 1995;
480 Spencer et al., 2012). For lakes in the study area having a long retention period (Table
481 S1), brackish lakes were found to have higher DOC concentrations (35.69 ± 43.52 mg
482 L^{-1}) compared with fresh lakes (7.94 ± 12.05 mg L^{-1}) (Table 1). Substantial variations
483 for both DOC and CDOM spectroscopic parameters were also observed between the
484 fresh and brackish lakes (ANOVA, $p < 0.05$) (Table 1 and Fig. 3). Previous investigations
485 have attributed this pattern to evapo-concentrated and accumulation processes in semi-
486 arid regions (Twardowski and Donaghay, 2002; Song et al., 2013; Wen et al., 2016).
487 However, the affined characteristics of brackish lakes in our study area could be due to
488 a weak connection between salinity (EC) and DOC (un-exhibited; $R^2=0.3$, t -test,
489 $p < 0.01$). Comparably, opposite results from brackish lakes in the northeastern plain
490 ($R^2= 0.93$, $p < 0.01$; Zhao et al., 2016) and on the Inner Mongolia Plateau ($R^2= 0.72$,
491 $p < 0.01$; Wen et al., 2016) have been previously noted. Generally, organic carbon with
492 different sources (allochthonous or autochthonous) and composition may result in
493 different relationships existing between DOC and salinity (EC) (Spencer et al., 2012).
494 This indicated that regional hydrogeological and climatic conditions may play an
495 important role in driving DOC variability in brackish lakes.

496 Although the lakes in the study area have high spatial heterogeneity, decreasing
497 salinity generally showed a consistent tendency of DOC concentrations (Fig. 2b).
498 Furthermore, salinity was divided into four groups ($>19\text{‰}$; $>7\text{‰}$; $>2\text{‰}$; $>1\text{‰}$) in
499 brackish lakes (Table 2). The normalized cumulative volume φ_i (φ_I , φ_{II} , φ_{IV} and φ_V) of
500 water samples with a salinity $>19\text{‰}$ (average EC $23764 \mu\text{s cm}^{-1}$) by EEM-FRI showed



501 moderate correlations with DOC concentrations (R^2 ranged from 0.52 to 0.73). R^2
502 correlation values showed a consistent decreasing tendency with salinity or EC. Based
503 on previous research which showed brackish lakes to always contain higher
504 concentrations of DOC than freshwater lakes in arid regions, this result may reflect
505 water residence times and DOM accumulation. DOM, along with other nutrients, could
506 accumulate via soil leaching and runoff passing through various landscapes (Song et al.,
507 2013). These DOM could be available for the microorganisms and sink to the bottom,
508 or be transformed into inorganic carbon (including CO_2) (Cole et al., 2007; Tranvik et
509 al., 2009). Increasing salinity (EC) could increase DOM solubility, resulting in an
510 impact on microbial activity due to a decrease of osmotic potential (Mavi et al., 2012).
511 Likewise, saturating small humic-like molecules formed colloidal particles which could
512 continue to form macromolecular structures (globular aggregates and ring-like) in high
513 ionic strength environments (Chin et al., 1998; Myneni et al., 1999; Zhao et al., 2016).
514 Therefore, DOC accumulates in brackish (terminal) waters at significantly higher rates
515 than those in fresh (open) waters (Duarte et al., 2005; Song et al., 2013).

516 A higher humic-like averaged percentage (P_V 60.2%) by normalized EEM-FRI
517 was presented in brackish lakes compared with freshwater lakes (51.8%) (Fig. 5),
518 signifying a greater formation of macromolecular structures of humic-like substances.
519 These processes could account for DOC and nutrients accumulating in terminal
520 brackish lakes. RDA results also indicated that environmental variables (CDOM
521 absorption and fluorescence) showed a relatively more positive correlation with water
522 quality in brackish lakes than in fresh lakes (Fig. 9). Zhao et al. (2016) reported that the
523 formed macromolecular structures of humic-like substances in brackish aquatic
524 environments can regulate the solubility of heavy metals and organic pollutants in water.
525 For areas of brackish lakes in the study site, elevated DOC concentrations could be



526 attributed to evapo-concentration and accumulation due to long residence times.

527 **4.2 The effect of solar radiation/ elevation**

528 In these synchronous processes (arid environment, terminal lakes and terrestrial inputs),
529 it is also important to highlight that these lakes receive higher levels of ultraviolet
530 radiation due to increasing altitude and a thin atmosphere compared to other studies
531 (Ren et al., 1997) (Fig. 1c). These attributes result in increased exposure to sunlight, an
532 increase in water residence times and strong UV radiation with an increase of altitude.
533 These factors may have an important influence on the photochemical oxidation
534 processes of DOC/CDOM and the mineralization of DOC (Duarte et al., 2005; Tobias
535 and Bohlke, 2011). Among the 63 lakes ($N=224$), the average $M(E_{250}:E_{365})$ (28.3 ± 20.3),
536 $S_{275-295}$ ($0.0380 \pm 0.009 \text{ nm}^{-1}$) and $SUVA_{254}$ ($1.47 \pm 2.55 \text{ mg C}^{-1} \text{ m}^{-1}$) in the brackish
537 lakes ($N=109$) were distinctly different from fresh lake results ($N=135$): $a(350)$ ($1.74 \pm$
538 1.99 m^{-1}), $M(E_{250}:E_{365})$ (16.27 ± 20.6), $S_{275-295}$ ($0.0324 \pm 0.01 \text{ nm}^{-1}$) and $SUVA_{254}$ (2.29
539 ± 1.36), respectively. This pattern is similar to that reported by Boehme et al. (2004) in
540 the Gulf of Mexico. In contrast with previous research indicating that brackish (terminal)
541 lakes always contain terrestrial DOM accumulation, our results show that they were
542 provided with low aromatic moieties of CDOM and average molecular weight of DOC
543 compared within fresh lakes (Helms et al., 2008; Gonnelli et al., 2013). Results also
544 highlighted significant differences in total fluorescence intensities ϕ_T between brackish
545 lakes ($1.44 \times 10^{10} \pm 8.1 \times 10^9 \text{ nm}$) and fresh lakes ($1.38 \times 10^{10} \pm 7.9 \times 10^9 \text{ nm}$) (ANOVA,
546 $p < 0.001$) (Fig. 5 and Fig. 6), respectively. However, we found that the average
547 normalized total fluorescence intensities ϕ_T between brackish lakes ($1.1 \times 10^9 \pm 8.8 \text{ QSU-}$
548 $\text{nm}^2 \cdot [\text{mg L}^{-1} \text{ C}]$) and fresh lakes ($3.3 \times 10^9 \pm 2.6 \text{ QSU-} \cdot \text{nm}^2 \cdot [\text{mg L}^{-1} \text{ C}]$) showed opposite
549 vitiation tendency when the ϕ_T was normalized to a DOC concentration of 1 mg L^{-1} .
550 This finding may account for relatively higher colorless DOC present in the brackish



551 lakes compared with the fresh lakes, a finding linked to solar radiation and prolonged
552 hydraulic retention time (Table S1).

553 In order to evaluate the influence of solar irradiance to CDOM optical
554 characteristics (Fig. 10), solar irradiance was divided into three groups (>2900 h; >2800
555 h; >2700 h) based on the consistent result of decreasing tendency between elevation
556 (solar radiation) and DOC concentration (Fig. 2). Strong solar radiance and time could
557 accelerate chromophores associated with high molecular weight being destroyed by
558 chemical bond rupture into low molecular weight pools in photolysis processes with a
559 prolonged hydraulic retention time and intensive solar radiation (McKnight et al., 2001).
560 However, for water samples with a solar radiance >2900 h (averaged solar irradiance),
561 DOC recorded a moderate positive correlation with $a(254)$ concentrations ($R^2=0.73$, t -
562 test, $p<0.01$), and a correlation with Fl_{370} ($R^2=0.50$, t -test, $p<0.01$). This indicated that,
563 in areas of the Tibet Plateau with intensive UV-B radiation (solar irradiance, >2900 h),
564 parts of the colored DOM (mainly from allochthonous inputs) have similar sources with
565 DOC. In addition, the PCA result of normalized cumulative volume φ_i by EEM-FRI in
566 this study exhibited that φ_{IV} (microbial protein-like) was consistent with φ_V (humic-like)
567 and φ_{III} (fuvic-like), signifying that they have common sources (Fig. 7). A positive
568 correlation between the total normalized cumulative volume $\varphi_{III&IV&V}$ and $\varphi_{I&II}$ ($R^2 =$
569 0.76 , $N= 109$; t -test, $p<0.01$) in brackish lakes also demonstrated that microbial protein-
570 like FDOM in these lakes had high DOC concentrations associated with products from
571 terrestrial microbial decomposition (Fig. 8d). Zhang et al. (2013) identified correlations
572 between total bacterial community structure and altitude in Tibet, and they did not found
573 more microorganism usually dominate in other lake environments, even though a
574 relative high average percentage of P_{IV} (brackish 15.8%; freshwater 13.3%) were
575 identified for normalized cumulative volume (Fig. 5). In the Tibet Plateau, intensive



576 solar radiance has the potential to enhance photochemical degradation of allochthonous
577 CDOM and high molecular weight CDOM, resulting in an increase in absorption
578 parameters with the production of low molecular weight CDOM. These findings are
579 contrary to those recorded from rivers in intermontane plateaus in the USA (Spencer et
580 al., 2012), lakes in the Songnen Plain, China (Song et al., 2013), Hulun Lake, China
581 (Wen et al., 2016) and basin rivers in China (Zhao et al., 2016). In arid and semi-arid
582 regions, brackish lakes commonly support highly active biological communities which
583 can actively break down refractory organic matter into DOC and accumulate in waters
584 (Wen et al., 2016). However, due to strong UV-B radiation and terminal lakes in the
585 Tibet Plateau, long sunlight duration may result in photobleaching of CDOM which
586 will limit microbial activities and increase mineralization of DOC (Granéli et al., 1996;
587 Duarte et al., 2005). These Characteristics characters result in CDOM and DOC in
588 brackish lakes in the study area being similar to that in marine environments. Zhang et
589 al. (2013) reported that the majority of lakes in Tibet were affiliated with SAR11-III
590 clade, similar to observations from Chesapeake Bay bacterio plankton. These findings
591 show that solar radiation has a non-negligible effect on CDOM photo-absorption
592 characteristics, and that it contributes to DOC variability and fate. In addition, a
593 comparatively prolonged hydraulic retention time (Duarte et al., 2005) and terrestrial
594 allochthonous inputs could cause higher DOC production and accumulation.

595 **[Insert Figure 10 about here]**

596 **4.3 Effects of land-cover variation on lakes**

597 Land-cover types within and around each lake affect soil runoff and leaching, having
598 an important effect on CDOM inputs and nutrient levels. These effects result in obvious
599 differences in physicochemical properties between the lakes (Bai et al., 2008; Heinz et



600 al., 2015; Song et al., 2013). In particular, for water samples dominated by
601 allochthonous substances in terminal lakes, spatial variations influenced terrestrial
602 inputs from soil and microbial activities due to plant decay. The land-cover in the basin
603 can also affect CDOM components and FDOM with similar climatic and hydrological
604 conditions. In order to acquire the integrated land-cover area of each basin, 20 basins
605 (B1-B20) were extracted using a 30 m resolution DEM (Digital Elevation Model;
606 <http://www.gscloud.cn/>). The proportion of different land use types to total basin area
607 is shown in Figure S2. In the Tibet Plateau, grass with plentiful organic-rich ecosystems
608 were the major land-cover types, accounting for amounts of total basin area (Fig. S2).
609 CDOM optical parameters of lake samples in each basin were averaged to analyze the
610 influence of land-cover, results showing a moderate correlation between DOC and
611 normalized humic-like ϕ_V for 20 basins ($R^2=0.54$, t -test, $p<0.01$; Fig. 11). Due to the
612 grass area accounting for amounts of basins (Fig. S3), normalized ϕ_{III} , ϕ_{IV} and ϕ_V in
613 basins with large grass areas (average area 14876 km²; $N=10$ basins) exhibited higher
614 values than in basins with small grass areas (averaged area 1976 km²; $N=10$ basins)
615 (ANOVA, $p<0.05$). Similar results were also found for forest and unused land, although
616 they accounted for small proportions of total area (Fig. 11). The Tibet Plateau is located
617 in an arid climatic zone with low rainfall, and the impoundment of lakes mainly depends
618 on surface runoff. Grasslands and forests were characterized by high nitrogen and
619 organic matter export rates (Bai et al., 2008; Heinz et al., 2015). High DOC
620 concentrations in the lake waters highlights the organic-rich nature of these ecosystems
621 (Zheng et al., 2015). As a result of climatic and geographical conditions, these
622 environment factors may change the optical characteristic of CDOM and water quality
623 in the Tibet Plateau.

624



625 **5. Conclusions**

626 Little is currently known about CDOM fluorescence and its relationship with water
627 quality in lakes across the Tibet Plateau. This area has a unique environmental condition
628 with strong ultraviolet radiation and low anthropogenic impact. In this study, EEM-FRI
629 was applied to characterize CDOM from 63 lakes ($N=244$) under spatial variation
630 between brackish lakes (salinity $>1\text{‰}$) and fresh lakes (salinity $<1\text{‰}$). Significant
631 differences of CDOM absorption parameters, normalized ϕ_T and DOC concentrations
632 were found between the two lake types (ANOVA, $p<0.05$), indicating lower average
633 molecular weight of DOM in brackish lakes.

634 Although the terrestrial component (ϕ_{III} and ϕ_V) accounted for large amounts of
635 fluorescence, PCA results indicated that the majority of microbial protein-like
636 fluorescence ϕ_{IV} of CDOM in the lakes derived from terrestrial microbial
637 decomposition products. This was attributed to DOC accumulation in terminal brackish
638 lakes having a prolonged hydraulic retention time and solar radiation. In addition,
639 correlations between average DOC concentrations and $a(254)$ in annual total sunshine
640 hours > 2900 h or salinity $>19\text{‰}$ (averaged EC, $23764\mu\text{s cm}^{-1}$) were identified, while
641 R^2 values of regression analysis had a decreasing tendency with sunshine hours and
642 salinity, respectively. Findings from our study also demonstrated that CDOM
643 components were affected by spatial variation in land-cover (mainly grass) (ANOVA,
644 $p<0.05$), with a moderate relationship between average normalized ϕ_V and DOC
645 concentration from 20 basins ($R^2=0.54$, t -test, $p<0.01$). These results demonstrate that
646 salinity, solar hours and land-cover may contribute to CDOM and DOC properties. The
647 EEM-FRI method was also shown to be very useful for evaluating the spatial dynamics
648 of FDOM components.

649 **Acknowledgments**



650 The research was jointly supported by the “One Hundred Talents” program from
651 Chinese Academy of Sciences, and the National Natural Science Foundation of China
652 (41730104). The authors thank all staff in Northeast Institute of Geography and
653 agricultural ecology of Chinese Academy of Sciences for their persistent assistance
654 with both field sampling and laboratory analysis. The authors also would like to thank
655 anonymous reviewers for their instructive and valuable comments that really
656 strengthened this manuscript.

657

658 **References**

659 APHA, AWWA and WEF,: Standard Methods for the Examination of Water and
660 Wastewater, American Public Health Association, Washington DC, 1998.

661 Arts, M. T., Robarts, R. D., Kasai, F., Waiser, M. J., Tumber, V. P., Plante, A. J., Rai,
662 H., and Lange, H. J.: The attenuation of ultraviolet radiation in high dissolved
663 organic carbon waters of wetlands and lakes on the northern Great Plains,
664 *Limnology and Oceanography*, 45(2), 292-299,
665 <https://doi.org/10.4319/lo.2000.45.2.0292>, 2000.

666 Baker, A.: Fluorescence excitation–Emission matrix characterization of some sewage-
667 impacted rivers, *Environmental Science &Technology*, 35(5), 948-953,
668 <https://doi.org/10.1021/es000177t>, 2001.

669 Battin, T. J., Luyssaert, S., Kaplan, L. A., Aufdenkampe, A. K., Richter, A., and Tranvik,
670 L. J.: The boundless carbon cycle, *Nature Geoscience*, 2(9), 598,
671 <https://doi.org/10.1038/ngeo618>, 2009.

672 Boehme, J., Coble, P., Conmy, R., and Stovall-Leonard, A.: Examining CDOM



- 673 fluorescence variability using principal component analysis: seasonal and regional
674 modeling of three-dimensional fluorescence in the Gulf of Mexico, *Marine*
675 *Chemistry*, 89(1-4), 3-14, <https://doi.org/10.1016/j.marchem.2004.03.019>, 2004.
- 676 Carlson, C. A., Hansell, D. A., and Tamburini, C. (Eds): DOC persistence and its fate
677 after export within the ocean interior, *Microbial Carbon Pump in the Ocean*, Jiao
678 N, Azam F, Sanders S, Washington DC, 57–59, 2011.
- 679 Chen, W., Westerhoff, P., Leenheer, J. A., and Booksh, K.: Fluorescence excitation-
680 emission matrix regional integration to quantify spectra for dissolved organic
681 matter, *Environmental science & technology*, 37(24), 5701-5710.
682 <https://doi.org/10.1021/es034354c>, 2003.
- 683 Chin, W. C., Orellana, M. V., and Verdugo, P.: Spontaneous assembly of marine
684 dissolved organic matter into polymer gels, *Nature*, 391(6667), 568,
685 <https://doi.org/10.1038/35345>, 1998.
- 686 Cole, J. J., Prairie, Y. T., Caraco, N. F., McDowell, W. H., Tranvik, L. J., Striegl, R. G.,
687 Duarte, C. M., Kortelainen, P., Downing, J. A., Middelburg, J. J., and Melack, J.:
688 Plumbing the global carbon cycle: integrating inland waters into the terrestrial
689 carbon budget, *Ecosystems*, 10(1), 172-185. [https://doi.org/10.1007/s10021-006-](https://doi.org/10.1007/s10021-006-9013-8)
690 [9013-8](https://doi.org/10.1007/s10021-006-9013-8), 2007.
- 691 Coble, P. G.: Characterization of marine and terrestrial DOM in seawater using
692 excitation-emission matrix spectroscopy, *Marine chemistry*, 51(4), 325-346,
693 [https://doi.org/10.1016/0304-4203\(95\)00062-3](https://doi.org/10.1016/0304-4203(95)00062-3), 1996.
- 694 Curtis, P. J., and Adams, H. E.: Dissolved organic matter quantity and quality from
695 freshwater and saltwater lakes in east-central Alberta, *Biogeochemistry*, 30(1), 59-
696 76, <https://doi.org/10.1007/BF02181040>, 1995.



- 697 Duarte, C. M., and Prairie, Y. T.: Prevalence of heterotrophy and atmospheric CO₂
698 emissions from aquatic ecosystems, *Ecosystems*, 8(7), 862-870,
699 <https://doi.org/10.1007/s10021-005-0177-4>, 2005.
- 700 Falkowski, P., Scholes, R. J., Boyle, E., Canadell, J., Canfield, D., Elser, J., Gruber, N.,
701 Hibbard, K., Högberg, P., Linder, S., Mackenzie, F. T., Moore III, B., Pedersen,
702 T., Rosenthal, Y., Seitzinger, S., Smetacek, V., and Steffen, W.: The global carbon
703 cycle: a test of our knowledge of earth as a system, *science*, 290(5490), 291-296,
704 <https://doi.org/10.1126/science.290.5490.291>, 2000.
- 705 Gonnelli, M., Vestri, S., and Santinelli, C.: Chromophoric dissolved organic matter and
706 microbial enzymatic activity. A biophysical approach to understand the marine
707 carbon cycle, *Biophysical chemistry*, 182, 79-85,
708 <https://doi.org/10.1016/j.bpc.2013.06.016>, 2013.
- 709 Granéli, W., Lindell, M., and Tranvik, L.: Photo-oxidative production of dissolved
710 inorganic carbon in lakes of different humic content, *Limnology and
711 Oceanography*, 41(4), 698-706, <https://doi.org/10.4319/lo.1996.41.4.0698>, 1996.
- 712 Hedges, J. I.: Global biogeochemical cycles: progress and problems, *Marine
713 chemistry*, 39(1-3), 67-93, [https://doi.org/10.1016/0304-4203\(92\)90096-S](https://doi.org/10.1016/0304-4203(92)90096-S), 1992.
- 714 Heinz, M., Graeber, D., Zak, D., Zwirnmann, E., Gelbrecht, J., and Pusch, M. T.:
715 Comparison of organic matter composition in agricultural versus forest affected
716 headwaters with special emphasis on organic nitrogen, *Environmental science &
717 technology*, 49, 2081-2090, <https://doi.org/10.1021/es505146h>, 2015.
- 718 Helms, J. R., Stubbins, A., Ritchie, J. D., Minor, E. C., Kieber, D. J., and Mopper, K.:
719 Absorption spectral slopes and slope ratios as indicators of molecular weight,
720 source, and photobleaching of chromophoric dissolved organic matter, *Limnology*



- 721 and Oceanography, 53(3), 955-969, <https://doi.org/10.4319/lo.2008.53.3.0955>,
- 722 2008.
- 723 Huguet, A., Vacher, L., Relexans, S., Saubusse, S., Froidefond, J.M., and Parlanti, E.:
724 Properties of fluorescent dissolved organic matter in the Gironde Estuary, Organic
725 Geochemistry, 40(6), 706-719, <https://doi.org/10.1016/j.orggeochem.2009.03.002>,
- 726 2009.
- 727 Kowalczyk, P., Cooper, W. J., Durako, M. J., Kahn, A. E., Gonsior, M., and Young, H.:
728 Characterization of dissolved organic matter fluorescence in the South Atlantic
729 Bight with use of PARAFAC model: Relationships between fluorescence and its
730 components, absorption coefficients and organic carbon concentrations, Marine
731 Chemistry, 118(1-2), 22-36, <https://doi.org/10.1016/j.marchem.2009.10.002>,
- 732 2010.
- 733 Jiao, N., Herndl, G. J., Hansell, D. A., Benner, R., Kattner, G., Wilhelm, S. W.,
734 Kirchman, D. L., Weinbauer, M. G., Luo, T., Chen, F., and Azam, F.: Microbial
735 production of recalcitrant dissolved organic matter: long-term carbon storage in
736 the global ocean, Nature Reviews Microbiology, 8(8), 593,
737 <https://doi.org/10.1038/nrmicro2386>, 2010.
- 738 Lawaetz, A. J., and Stedmon, C. A.: Fluorescence intensity calibration using the Raman
739 scatter peak of water, Applied spectroscopy, 63(8), 936-940,
740 <https://doi.org/10.1366/000370209788964548>, 2009.
- 741 Liu, X., and Chen, B.: Climatic warming in the Tibetan Plateau during recent decades,
742 International journal of climatology, 20(14), 1729-1742,
743 [https://doi.org/10.1002/1097-0088\(20001130\)20:14<1729::AID-](https://doi.org/10.1002/1097-0088(20001130)20:14<1729::AID-JOC556>3.0.CO;2-Y)
744 [JOC556>3.0.CO;2-Y](https://doi.org/10.1002/1097-0088(20001130)20:14<1729::AID-JOC556>3.0.CO;2-Y), 2000.



- 745 Mavi, M. S., Marschner, P., and Chittleborough, D. J.: Salinity and sodicity affect soil
746 respiration and dissolved organic matter dynamics differentially in soils varying
747 in texture, *Soil biology and biochemistry*, 45, 8-13,
748 <https://doi.org/10.1016/j.soilbio.2011.10.003>, 2012.
- 749 McKnight, D. M., Boyer, E. W., Westerhoff, P. K., Doran, P. T., Kulbe, T., and
750 Andersen, D. T.: Spectrofluorometric characterization of dissolved organic matter
751 for indication of precursor organic material and aromaticity, *Limnology and*
752 *Oceanography*, 46(1), 38-48, <https://doi.org/10.4319/lo.2001.46.1.0038>, 2001.
- 753 Myneni, S. C. B., Brown, J. T., Martinez, G. A., and Meyer-Ilse, W.: Imaging of humic
754 substance macromolecular structures in water and soils, *Science*, 286(5443),
755 1335-1337, <https://doi.org/10.1126/science.286.5443.1335>, 1999.
- 756 Qin, J., Yang, K., Liang, S., and Guo, X.: The altitudinal dependence of recent rapid
757 warming over the Tibetan Plateau, *Climatic Change*, 97(1-2), 321,
758 <https://doi.org/10.1007/s10584-009-9733-9>, 2009.
- 759 Ran, L. S., X. X. Lu, H. G. Sun, Han, J. T., Li, R. H., and Zhang, J.M.: Spatial and
760 seasonal variability of organic carbon transport in the Yellow River, China,
761 *Journal of Hydrology*, 498, 76-88, <https://doi.org/10.1016/j.jhydrol.2013.06.018>,
762 2013.
- 763 Ren, P. B. C., Sigernes, F., and Gjessing, Y.: Ground-based measurements of solar
764 ultraviolet radiation in Tibet: Preliminary results, *Geophysical research*
765 *letters*, 24(11), 1359-1362, <https://doi.org/10.1029/97GL01319>, 1997.
- 766 Singh, S., D'Sa, E. J., and Swenson, E. M.: Chromophoric dissolved organic matter
767 (CDOM) variability in Barataria Basin using excitation–emission matrix (EEM)



768 fluorescence and parallel factor analysis (PARAFAC), *Science of the total*
769 *environment*, 408(16), 3211-3222,
770 <https://doi.org/10.1016/j.scitotenv.2010.03.044>, 2010.

771 Song, K. S., Zang, S. Y., Zhao, Y., Li, L., Du, J., Zhang, N. N., Wang, X. D., Shao, T.
772 T., Guan, Y., and Liu, L.: Spatiotemporal characterization of dissolved carbon for
773 inland waters in semi-humid/semi-arid region, China, *Hydrology and Earth*
774 *System Sciences*, 17(10), 4269-4281, <https://doi.org/10.5194/hess-17-4269-2013>,
775 2013.

776 Song, K., Wang, M., Du, J., Yuan, Y., Ma, J. H., Wang, M., and Mu, G. Y.:
777 Spatiotemporal variations of lake surface temperature across the Tibetan Plateau
778 using MODIS LST product, *Remote Sensing*, 8(10), 854,
779 <https://doi.org/10.3390/rs8100854>, 2016.

780 Spencer, R. G., Butler, K. D., and Aiken, G. R.: Dissolved organic carbon and
781 chromophoric dissolved organic matter properties of rivers in the USA, *Journal of*
782 *Geophysical Research: Biogeosciences*, 117(G3), G03001,
783 <https://doi.org/10.1029/2011JG001928>, 2012.

784 Stedmon, C. A., Markager, S., and Bro, R.: Tracing dissolved organic matter in aquatic
785 environments using a new approach to fluorescence spectroscopy, *Marine*
786 *Chemistry*, 82(3-4), 239-254, [https://doi.org/10.1016/S0304-4203\(03\)00072-0](https://doi.org/10.1016/S0304-4203(03)00072-0),
787 2003.

788 Tranvik, L. J., Downing, J. A., Cotner, J. B., Loiselle, S. A., Striegl, R. G., Ballatore,
789 T. J., Dillon, P., Finlay, K., Fortino, K., Knoll, L. B., Kortelainen, P. L., Kutser,
790 T., Larsen, S., Laurion, I., Leech, D. M., McCallister, S. L., McKnight, D. M.,
791 Melack, J. M., Overholt, E., Porter, J. A., Prairie, Y., Renwick, W. H., Roland, F.,



- 792 Sherman, B. S., Schindler, D. W., Sobek, S., Tremblay, A., Vanni, M. J.,
793 Verschoor, A. M., Wachenfeldt, E. V., and Weyhenmeyer, G. A.: Lakes and
794 reservoirs as regulators of carbon cycling and climate, *Limnology and*
795 *Oceanography*, 54(6part2), 2298-2314,
796 https://doi.org/10.4319/lo.2009.54.6_part_2.2298, 2009.
- 797 Tobias, C., and Böhlke, J. K.: Biological and geochemical controls on diel dissolved
798 inorganic carbon cycling in a low-order agricultural stream: Implications for reach
799 scales and beyond, *Chemical Geology*, 283(1-2), 18-30,
800 <https://doi.org/10.1016/j.chemgeo.2010.12.012>, 2011.
- 801 Twardowski, M. S., and Donaghay, P. L.: Photobleaching of aquatic dissolved
802 materials: Absorption removal, spectral alteration, and their interrelationship,
803 *Journal of Geophysical Research: Oceans*, 107(C8), 6-1-6-12,
804 <https://doi.org/10.1029/1999JC000281>, 2002.
- 805 Waiser, M. J., and Robarts, R. D.: Changes in composition and reactivity of
806 allochthonous DOM in a prairie saline lake, *Limnology and Oceanography*, 45(4),
807 763-774, <https://doi.org/10.4319/lo.2000.45.4.0763>, 2000.
- 808 Weishaar, J. L., Aiken, G. R., Bergamaschi, B. A., Fram, M. S., Fujii, R., and Mopper,
809 K.: Evaluation of specific ultraviolet absorbance as an indicator of the chemical
810 composition and reactivity of dissolved organic carbon, *Environmental science &*
811 *technology*, 37(20), 4702-4708, <https://doi.org/10.1021/es030360x>, 2003.
- 812 Wen, Z. D., Song, K. S., Zhao, Y., Du, J., and Ma, J. H.: Influence of environmental
813 factors on spectral characteristics of chromophoric dissolved organic matter
814 (CDOM) in Inner Mongolia Plateau, China, *Hydrology and Earth System Sciences*,
815 20(2), 787, <https://doi.org/10.5194/hess-20-787-2016>, 2016.



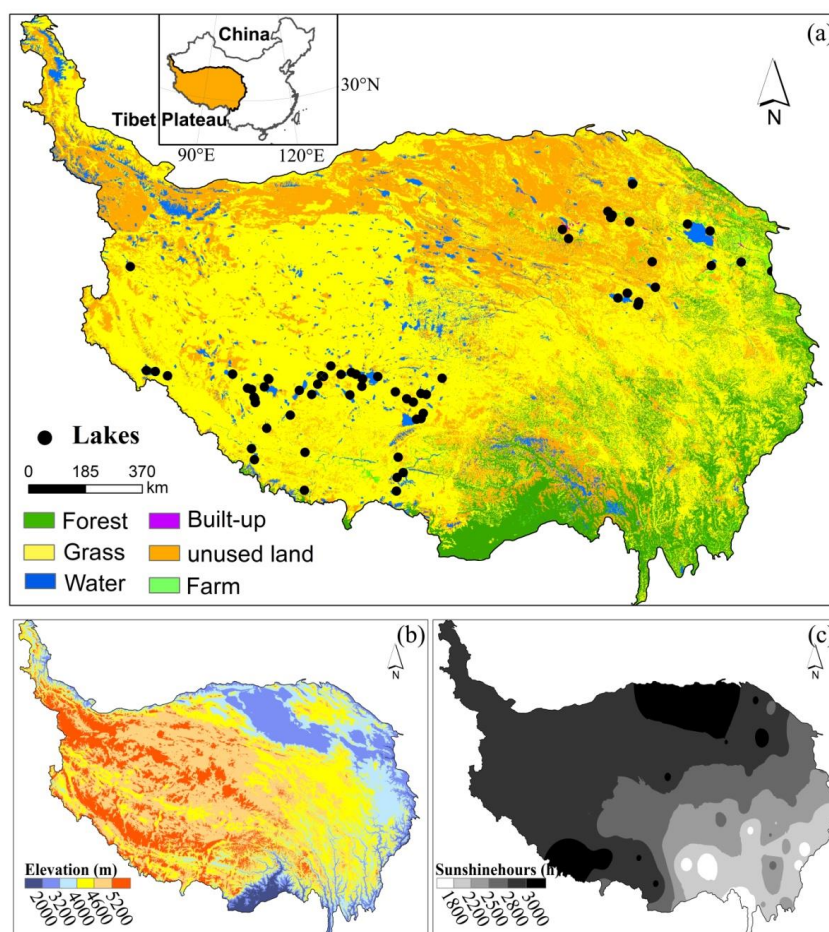
- 816 Yao, X., Y. L. Zhang, G. W. Zhu, Qin, B. Q., Feng, L. Q., Cai, L. L., and Gao, G.:
817 Resolving the variability of CDOM fluorescence to differentiate the sources and
818 fate of DOM in Lake Taihu and its tributaries, *Chemosphere*, 82, 145-155,
819 <https://doi.org/10.1016/j.chemosphere.2010.10.049>, 2011.
- 820 Yamashita, Y., Maie, N., Briceno, H., and Jaffé, R.: Optical characterization of
821 dissolved organic matter in tropical rivers of the Guayana Shield, Venezuela,
822 *Journal of Geophysical Research: Biogeosciences*, 115(G1),
823 <https://doi.org/10.1029/2009JG000987>, 2010.
- 824 Zhang, R., Wu, Q., Piceno, Y. M., Desantis, T. Z., Saunders, F. M., Andersen, G. L.,
825 and Liu, W. T.: Diversity of bacterioplankton in contrasting Tibetan lakes revealed
826 by high-density microarray and clone library analysis, *FEMS microbiology*
827 *ecology*, 86(2), 277-287, <https://doi.org/10.1111/1574-6941.12160>, 2013.
- 828 Zhang, G., Xie, H., Kang, S., Yi, D., and Ackley, S. F.: Monitoring lake level changes
829 on the Tibetan Plateau using ICESat altimetry data (2003–2009), *Remote Sensing*
830 *of Environment*, 115(7), 1733-1742, <https://doi.org/10.1016/j.rse.2011.03.005>,
831 2011.
- 832 Zhang, Y., Yin, Y., Feng, L., Zhu, G., Shi, Z., Liu, X., and Zhang, Y.: Characterizing
833 chromophoric dissolved organic matter in Lake Tianmuhu and its catchment basin
834 using excitation-emission matrix fluorescence and parallel factor analysis, *Water*
835 *research*, 45(16), 5110-5122, <https://doi.org/10.1016/j.watres.2011.07.014>, 2011.
- 836 Zhang, Y. L., E. L. Zhang, Y. Yin, Dijk, M. A.V., Feng, L. Q., Shi, Z. Q., Liu, M. L.,
837 and Qin, B. Q.: Characteristics and sources of chromophoric dissolved organic
838 matter in lakes of the Yungui Plateau, China, differing in trophic state and altitude,
839 *Limnology and Oceanography*, 55, 2645–2659,



- 840 <https://doi.org/10.4319/lo.2010.55.6.2645>, 2010.
- 841 Zhao, Y., Song, K., Shang, Y., Shao, T., Wen, Z., and Lv, L.: Characterization of
842 CDOM of river waters in China using fluorescence excitation-emission matrix and
843 regional integration techniques, *Journal of Geophysical Research: Biogeosciences*,
844 122(8): 1940-1953, <https://doi.org/10.1002/2017JG003820>, 2017.
- 845 Zhao, Y., Song, K., Wen, Z., Li, L., Zang, S., Shao, T., Li, S., and Du, J.: Seasonal
846 characterization of CDOM for lakes in semiarid regions of Northeast China using
847 excitation–emission matrix fluorescence and parallel factor analysis (EEM–
848 PARAFAC), *Biogeosciences*, 13(5), 1635-1645, [https://doi.org/10.5194/bg-13-](https://doi.org/10.5194/bg-13-1635-2016)
849 1635-2016, 2016.
- 850 Zhou, Y., Jeppesen, E., Zhang, Y., Shi, K., Liu, X., and Zhu, G.: Dissolved organic
851 matter fluorescence at wavelength 275/342 nm as a key indicator for detection of
852 point-source contamination in a large Chinese drinking water lake, *Chemosphere*,
853 144, 503-509, <https://doi.org/10.1016/j.chemosphere.2015.09.027>, 2016.
- 854
- 855
- 856
- 857



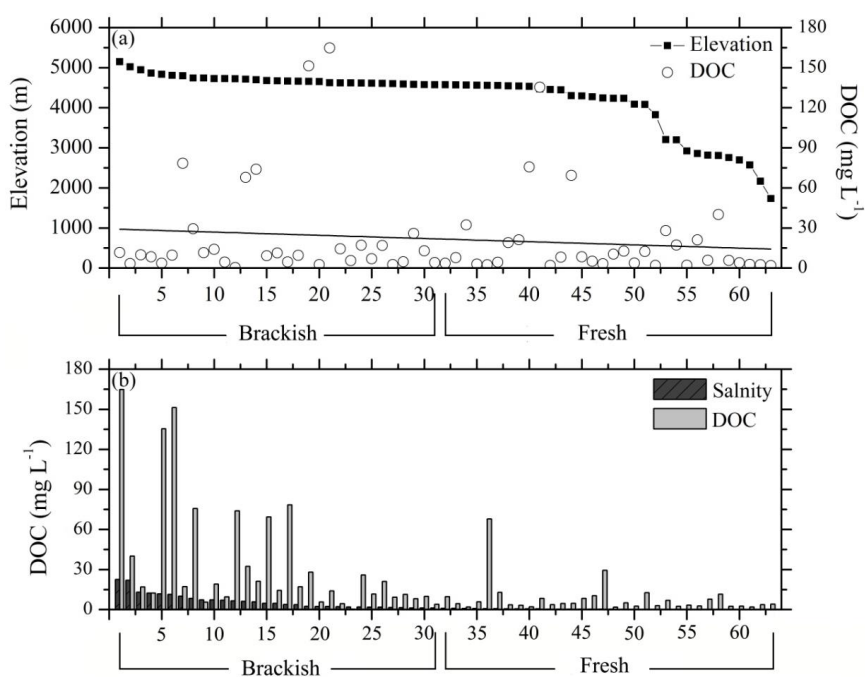
858 **Figure 1 (a)** Map of sampling locations from lakes in Tibet Plateau with various land
859 use/land cover types; (b) the elevation (m) of Tibet Plateau; (c) sunshine duration
860 characteristics for the Tibet Plateau. The total sunshine hours in 2016 were from China
861 meteorological data sharing service system.



862



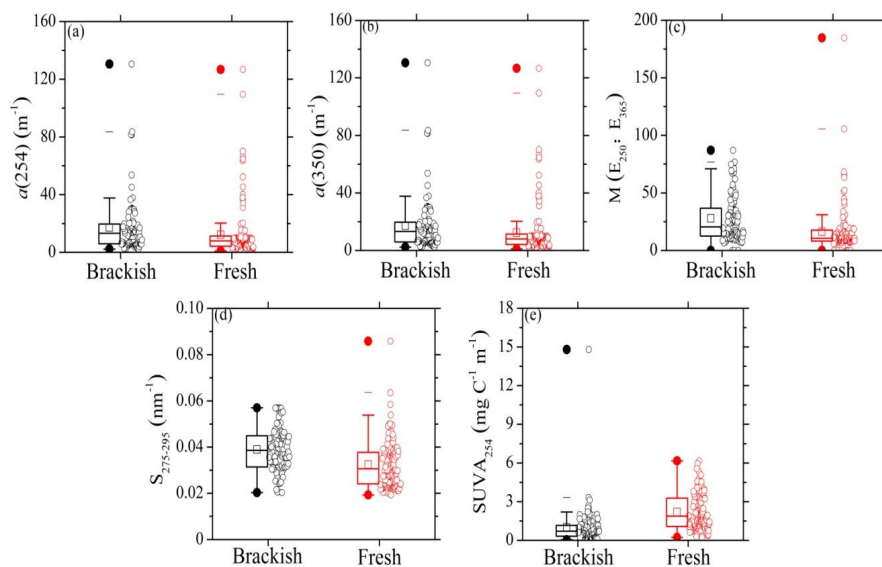
863 **Figure 2** The DOC, salinity and elevation from 63 lakes collected in Tibet Plateau, (a)
 864 The elevation (m) of 63 lakes in Tibet Plateau and corresponding DOC concentrations,
 865 and (b) Mean DOC and salinity (EC) of 63 lakes. The full line represents the tendency
 866 linear equation of average DOC concentrations. The numbers was the lake name
 867 according to Table S1.



868



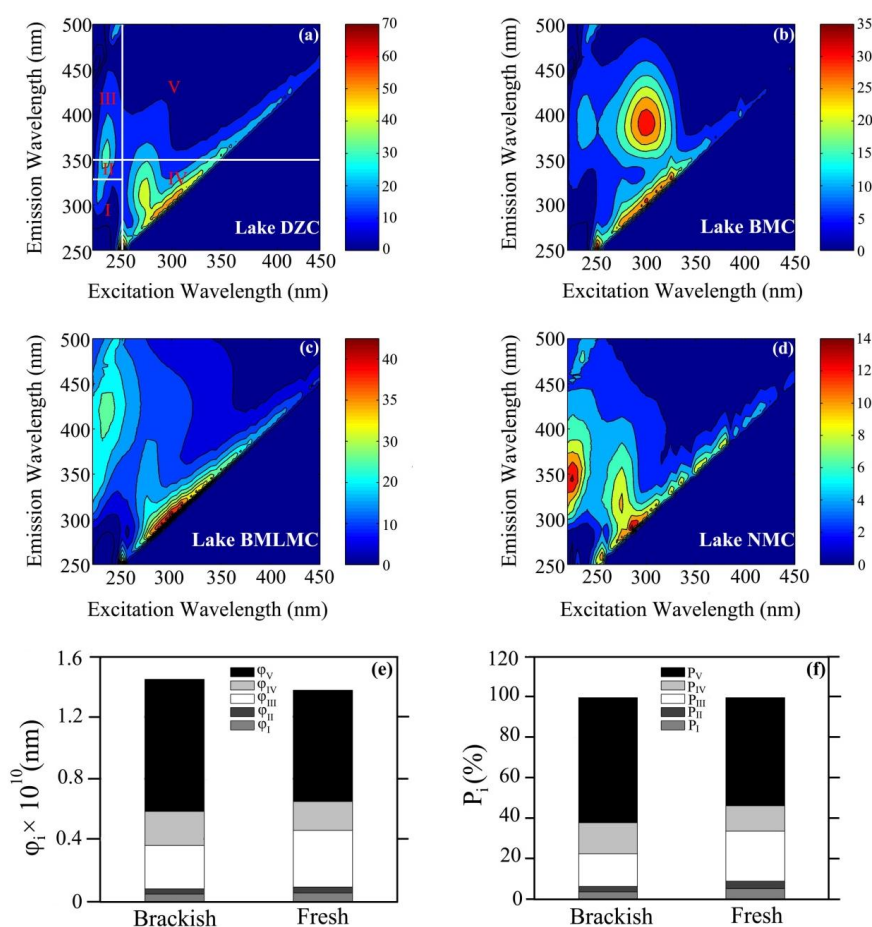
869 **Figure 3.** Box plots of $a(254)$ (a), $a(350)$ (b), $M(E_{250}: E_{365})$ (c), $S_{275-295}$ (d) and $SUVA_{254}$
870 (d) for brackish and fresh waters in the Tibet Plateau. The black line and the hollow
871 squares represent the median and mean values, respectively. The horizontal edges of
872 the boxes denote the 25th and 75th percentiles; the whiskers denote the 10th and 90th
873 percentiles. The black circles represent samples of brackish lakes, and red were fresh
874 lakes. Then the unit of $SUVA_{254}$ is $\text{mg C}^{-1} \text{m}^{-1}$, $S_{275-295}$ is nm^{-1} , and CDOM absorption
875 at 254 nm and 350 nm is m^{-1} .



876



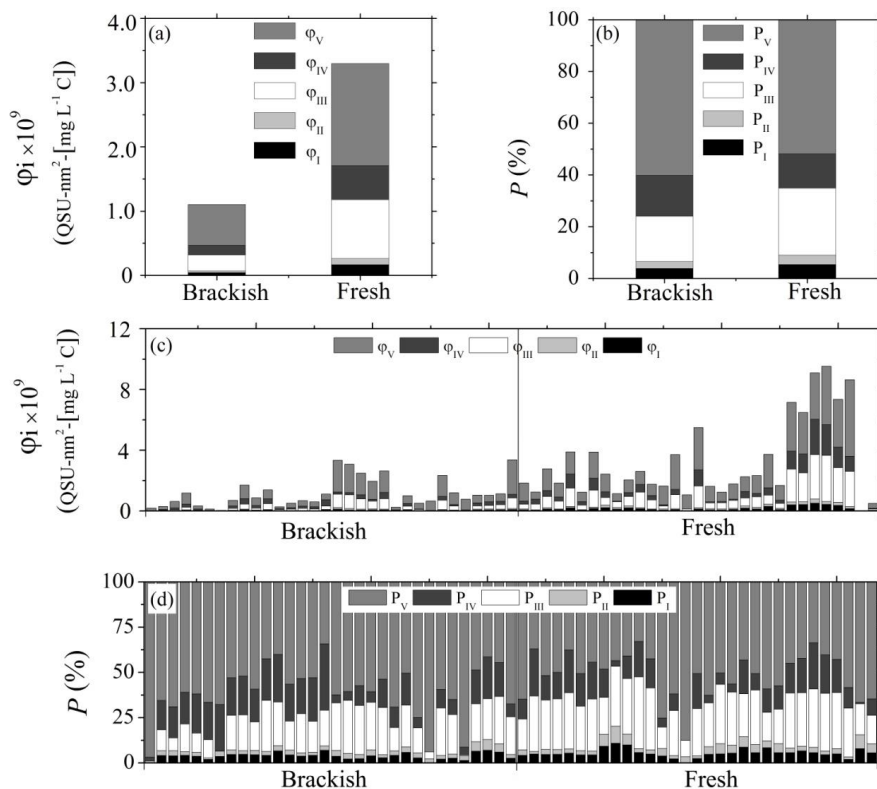
877 **Figure 4.** Four typical EEM fluorescence spectra (a-d) and FRI results, (a) Lake DZC,
 878 (b) Lake BMC, (c) Lake BMLMC, (d) Lake NMC, (e) The proportion and cumulative
 879 volume proportion of EEMFRI-extracted average FDOM components from five
 880 regions in brackish lakes and fresh lakes in Tibet Plateau and (f) distributions of
 881 percentages of EEM-FRI extracted FDOM.



882



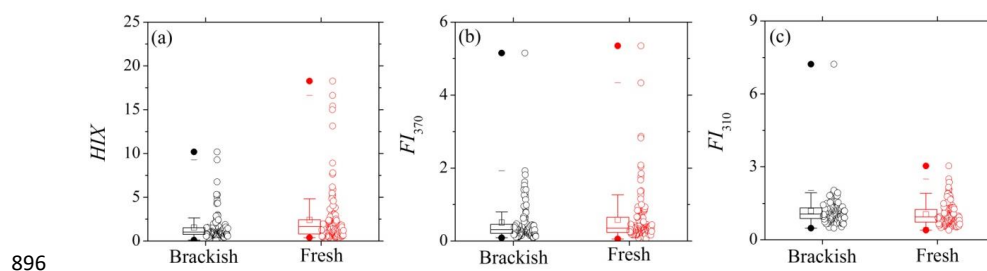
883 **Figure 5.** Normalized EEM-FRI fluorescence component and spatial characteristics
 884 from 63 lakes in Tibet Plateau, (a) normalized cumulative volume ϕ_i of EEM-FRI
 885 extracted average FDOM components from five regions in brackish lakes and fresh
 886 lakes, (b) percentages P_i of EEM-FRI extracted FDOM in brackish lakes and fresh lakes,
 887 (c) spatial distributions of normalized cumulative volume ϕ_i in brackish lakes and fresh
 888 lakes and (d) spatial distributions of percentages P_i of EEM-FRI extracted FDOM in
 889 brackish lakes and fresh lakes.



890

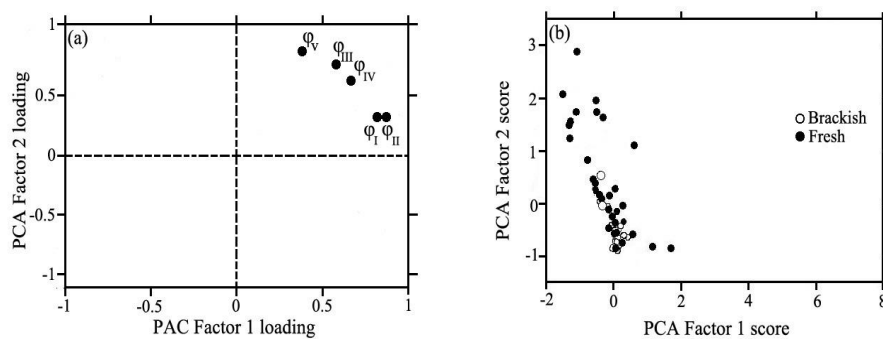


891 **Figure 6.** Box plots of HIX (a), FI_{370} (b) and FI_{310} (c) for brackish and fresh waters in
 892 the Tibet Plateau. The black line and the hollow squares represent the median and mean
 893 values, respectively. The horizontal edges of the boxes denote the 25th and 75th
 894 percentiles; the whiskers denote the 10th and 90th percentiles. The black circles
 895 represent samples of brackish lakes, and red were fresh lakes.





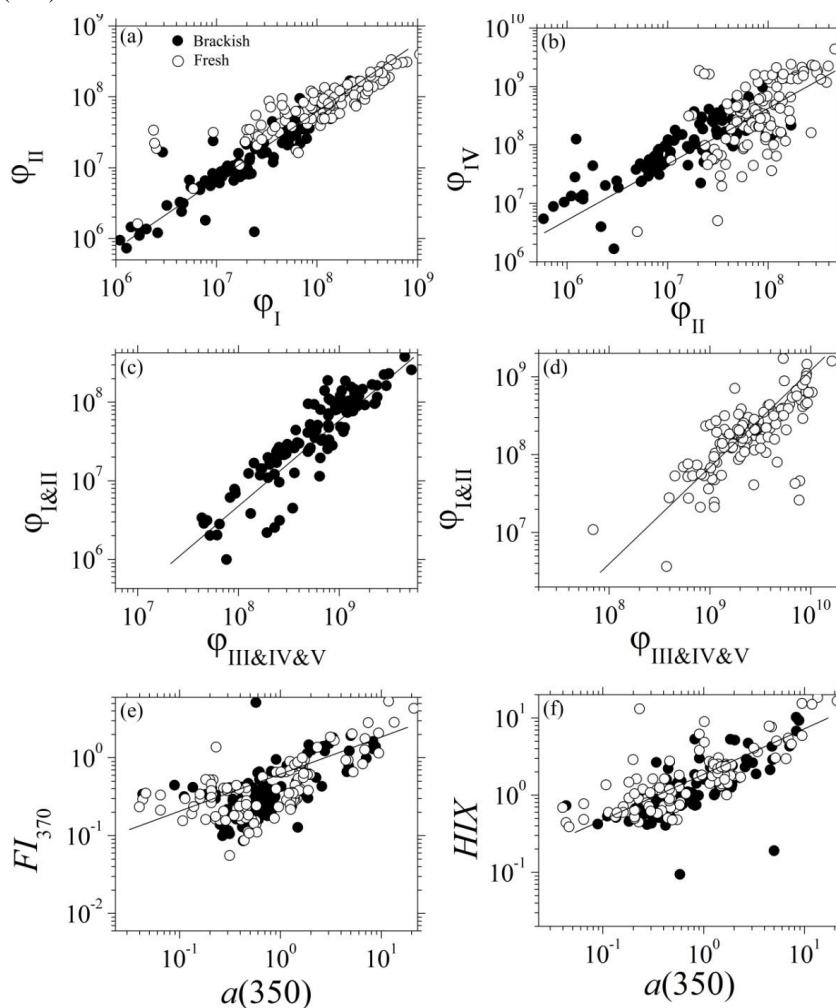
897 **Figure 7.** Principal component analysis (PCA) results of normalized cumulative
 898 volume φ_i by EEM-FRI. (a) Loadings of PCA factors and (b) property-property plots
 899 of PCA factor scores of 63 lakes. The unit of normalized cumulative volume φ_i ($i=I, II,$
 900 III, IV, V) is $QSU\text{-}nm^2\text{-}[mg L^{-1} C]$.



901



902 **Figure 8.** The correlations between normalized cumulative volume ϕ_I and ϕ_{II} by EEM-
903 FRI for water samples in brackish lakes and fresh lakes (a); the correlations between
904 normalized ϕ_I and ϕ_{IV} (b); the correlations between normalized ϕ_{II} and ϕ_{IV} (c); the
905 correlations between normalized $\phi_{III\&IV\&V}$ and $\phi_{I\&II}$ by EEM-FRI (d); the correlations
906 between $a(350)$ and FI_{370} (e), and the correlations between $a(350)$ and HIX (f). The unit
907 of normalized cumulative volume ϕ_i ($i=I, II, III, IV, V$) is $QSU\cdot nm^2\cdot [mg\ L^{-1}\ C]$, and
908 $a(350)$ was nm^{-1} .

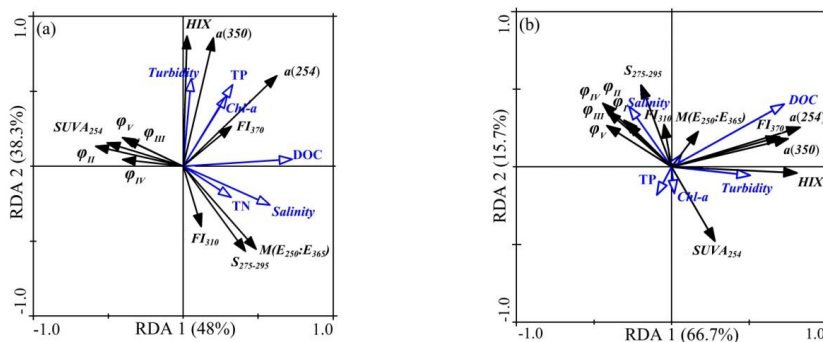


909



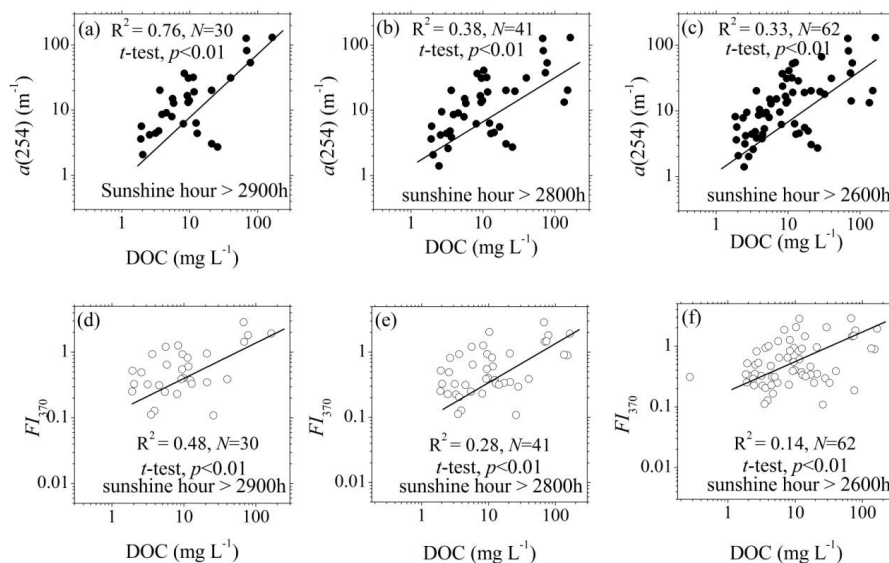
910 **Figure 9.** Redundancy analysis (RDA) of CDOM spectroscopic parameters and the
 911 water quality parameters in (a) brackish lakes and (b) fresh lakes Tibetan Plateau. φ_i
 912 was deleted due to large inflation factor (>20). The solid arrows and black font represent
 913 the environmental explanatory variables, and hollow arrows and blue fonts were species
 914 variables, respectively. (c) and (d) are the correlation between $a(254)$, DOC and FI_{370}
 915 in brackish and fresh lakes. The unit of TN, TP and DOC was mg L^{-1} ; Chl-*a* was $\mu\text{g L}^{-1}$;
 916 salinity is ‰; turbidity is NTU (nephelometric turbidity unit). Then the unit of $a(254)$
 917 and $a(350)$ is m^{-1} ; $SUVA_{254}$ is $\text{L mg C}^{-1} \text{m}^{-1}$; φ_i ($i=I, II, III, IV, V$) is $\text{QSU-nm}^{-2}\text{-}[\text{mg L}^{-1}$
 918 $\text{C}]$.

919





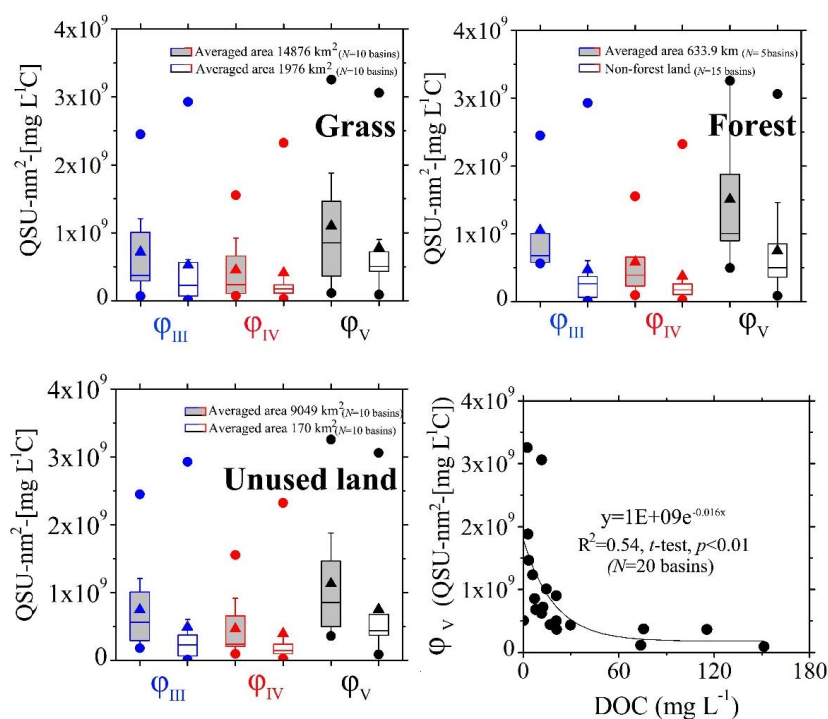
920 **Figure 10.** The correlation between average DOC concentrations and $a(254)$ in annual
921 total sunshine hours > 2900h (a), annual total sunshine hours > 2800h (b) and annual
922 total sunshine hours > 2600h (c). Then the correlation between average DOC
923 concentrations and FI_{370} in annual total sunshine hours > 2900h (d), annual total
924 sunshine hours > 2800h (e) and annual total sunshine hours > 2600h (f). The annual
925 total sunshine hours in Tibet are from the China metrological data sharing service
926 system.



927



928 **Figure 11.** (a) Box plots of normalized ϕ_{III} , ϕ_{IV} and ϕ_V in basins with large grass area
 929 (averaged area 14876 km²; $N=10$ basins, B1, B10, B19, B2, B11, B17, B12, B5, B20,
 930 B14), and basins with small grass area (averaged area 1976 km²; $N=10$ basins, B4, B6,
 931 B8, B9, B3, B15, B18, B16, B13, B17). (b) Box plots of normalized ϕ_{III} , ϕ_{IV} and ϕ_V in
 932 basins with large forest area (averaged area 633.9 km²; $N=5$ basins, B2, B1 B4, B11,
 933 B10), and in non-forest land. (c) Box plots of normalized ϕ_{III} , ϕ_{IV} and ϕ_V in basins with
 934 large unused land area (averaged area 9049 km²; $N=10$ basins, B1, B4, B2, B17, B3,
 935 B10, B11, B20, B19, B12), and basins with small grass area (averaged area 170 km²;
 936 $N=10$ basins, B6, B14, B8, B9, B15, B16, B7, B13, B5, B18). The black line and the
 937 hollow squares represent the median and mean values, respectively. The horizontal
 938 edges of the boxes denote the 25th and 75th percentiles; the whiskers denote the 10th
 939 and 90th percentiles. (d) The correlation between DOC and normalized humic like ϕ_V
 940 of 20 basins in Tibet Plateau.



941

942


 943 **Table 1** Water quality parameters of samples from 63 lakes ($N=244$) in Tibet Plateau

Parameters	Brackish Lakes ($N=109$)		Fresh Lakes ($N=135$)	
	Mean	Max-Min	Mean	Max-Min
Turbidity	14.63±24.40	0-87.78	16.7±43.61	0-212.51
EC	8880.23±8235.912	1673-33141.2	536.55±332.29	120.1-1369.2
Salinity	6.01±5.60	1.14-22.54	0.36±0.22	0.08-0.93
TN	4.54±4.32	0.31-15.56	2.31±2.64	0.16-10.15
TP	0.45±1.35	0.006-6.79	0.04±0.03	0.001-0.08
Chl-a	2.57±5.73	0-31.37	1.4±2.68	0.09-14.68
DOC	35.69±43.52	0.27-164.8	7.94±12.17	1.84-67.79

944 TN, TP, DOC, DTC, and DIC represent total nitrogen, total phosphorus, dissolved organic carbon,
 945 dissolved total carbon and dissolved inorganic carbon concentrations, respectively (mg L^{-1}). EC
 946 represents the electrical conductivity of water samples ($\mu\text{s cm}^{-1}$). Chl-a, chlorophyll-a concentration
 947 ($\mu\text{g L}^{-1}$). The unit of turbidity is NTU, nephelometric turbidity unit, and salinity is ‰.



948 **Table 2** Regression analysis equations of DOC concentration and normalized cumulative volume φ_i
 949 ($i=I, II, III, IV, V$) for all the water samples from 63 lakes ($N=244$) in Tibet Plateau

Salinity	Averaged EC	Regression equation	R ²
DOC & φ_I (Tyrosine like)			
>19	23764	$y=3E+07e^{-0.013x}$, ($N=29$)	0.73
>7	10945	$y=3E+07e^{-0.014x}$, ($N=64$)	0.42
>2	5708	$y=3E+07e^{-0.014x}$, ($N=84$)	0.34
>1	2119	$y=4E+07e^{-0.015x}$, ($N=109$)	0.34
<1	586	$y = 1E+08e^{-0.034x}$, ($N=135$)	0.03
DOC & φ_{II} (Tryptophan like)			
>19	23764	$y=1E+07e^{-0.009x}$, ($N=29$)	0.64
>7	10945	$y=2E+07e^{-0.012x}$, ($N=64$)	0.41
>2	5708	$y=2E+07e^{-0.012x}$, ($N=84$)	0.34
>1	2119	$y=2E+07e^{-0.014x}$, ($N=109$)	0.34
<1	586	$y = 8E+07e^{-0.023x}$, ($N=135$)	0.03
DOC & φ_{III} (Fulvic like)			
>19	23764	$y = 9E+07e^{-0.009x}$, ($N=29$)	0.30
>7	10945	$y = 1E+08e^{-0.01x}$, ($N=64$)	0.15
>2	5708	$y = 2E+08e^{-0.01x}$, ($N=84$)	0.08
>1	2119	$y = 2E+08e^{-0.01x}$, ($N=109$)	0.08
<1	586	$y = 7E+08e^{-0.023x}$, ($N=135$)	0.02
DOC & φ_{IV} (Microbial protein like)			
>19	23764	$y=1E+08 e^{-0.010x}$, ($N=29$)	0.52
>7	10945	$y=1E+08 e^{-0.012x}$, ($N=64$)	0.37
>2	5708	$y=1E+08 e^{-0.012x}$, ($N=84$)	0.27
>1	2119	$y=1E+08 e^{-0.012x}$, ($N=109$)	0.28
<1	586	$y = 4E+08e^{-0.034x}$, ($N=135$)	0.02
DOC & φ_V (Humic like)			
>19	23764	$y=4E+08 e^{-0.008x}$, ($N=29$)	0.59
>7	10945	$y=4E+08 e^{-0.009x}$, ($N=64$)	0.28
>2	5708	$y=4E+08 e^{-0.009x}$, ($N=84$)	0.23
>1	2119	$y=5E+08 e^{-0.010x}$, ($N=109$)	0.25
<1	586	$y = 2E+09e^{-0.02x}$, ($N=135$)	0.03
DOC & $\varphi_{III&VI&V}$ (Humic like& Microbial protein like & Fulvic like)			
>19	23764	$y = 5E+08e^{-0.009x}$, ($N=29$)	0.58
>7	10945	$y = 6E+08e^{-0.01x}$, ($N=64$)	0.30



>2	5708	$y = 7E+08e^{-0.01x}$, ($N=84$)	0.24
>1	2119	$y = 8E+08e^{-0.011x}$, ($N=109$)	0.26
<1	586	$y = 3E+09e^{-0.025x}$, ($N=135$)	0.03

DOC & $\phi_{I&II}$ (Tyrosine like & Tryptophan like)

>19	23764	$y = 4E+07e^{-0.013x}$, ($N=29$)	0.74
>7	10945	$y = 5E+07e^{-0.014x}$, ($N=64$)	0.45
>2	5708	$y = 5E+07e^{-0.014x}$, ($N=84$)	0.32
>1	2119	$y = 6E+07e^{-0.015x}$, ($N=109$)	0.34
<1	586	$y = 2E+08e^{-0.03x}$, ($N=135$)	0.03

950 The unit of EC is $\mu\text{s cm}^{-1}$; salinity is ‰; DOC concentration is mg L^{-1} ; ϕ_i ($i=I, II, III, IV, V$) is QSU-
951 $\text{nm}^2\text{-}[\text{mg L}^{-1} \text{ C}]$.